ACTA TECNOLOGÍA

electronic journal
ISSN 2453-675X
Volume 5
Issue 4
2019

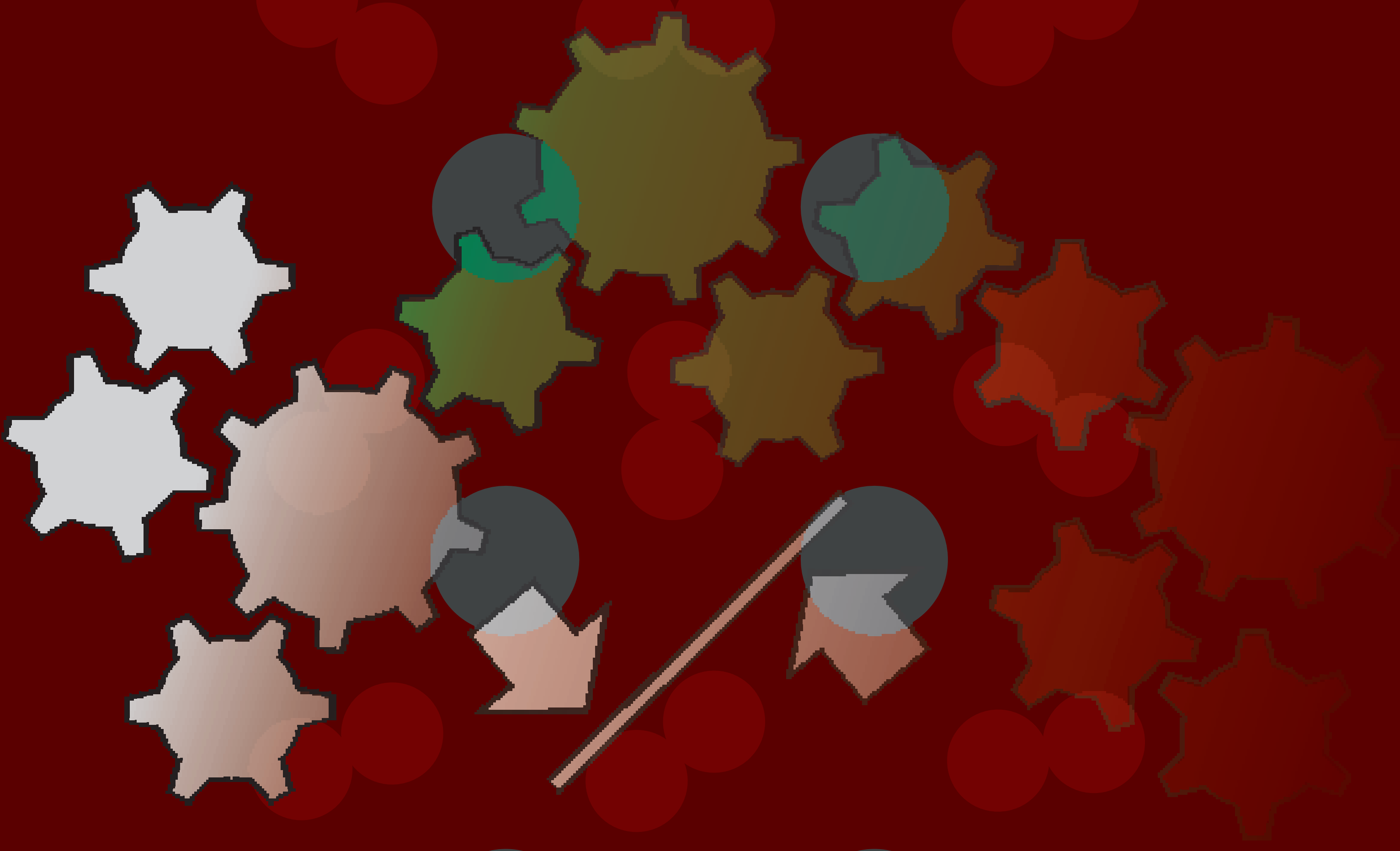

International Scientific Journal about Technologies

CONTENTS

(DECEMBER 2019)

doi:10.22306/atec.v5i4.53

Received: 30 Apr. 2019
Accepted: 21 May 2019

ALTERNATIVE APPLICATIONS OF PELTIER THERMOPILES IN COOLING METAL HYDRIDE CONTAINERS

Tomáš Brestovič
Department of Power Engineering, Technical university of Košice, Letná 9, 042 00 Košice, Slovak Republic, EU, tomas.brestovic@tuke.sk (corresponding author)
Natália Jasminská
Department of Power Engineering, Technical university of Košice, Letná 9, 042 00 Košice, Slovak Republic, EU, natalia.jasminska@tuke.sk
Marián Lázár
Department of Power Engineering, Technical university of Košice, Letná 9, 042 00 Košice, Slovak Republic, EU, marian.lazar@tuke.sk
Ľubica Bednárová
Department of Power Engineering, Technical university of Košice, Letná 9, 042 00 Košice, Slovak Republic, EU, lubica.bednarova@tuke.sk

Keywords: Peltier thermopile, cooling, metal hydride container, absorption, hydrogen

Abstract: Hydrogen absorption into a metal hydride container is accompanied with generation of heat that must be removed during the process. In the case that the container is not cooled, the gas pressure rapidly increases and even with a small amount of stored hydrogen it exceeds the permissible value. Peltier thermopiles offer an interesting alternative to conventional cooling methods and they have been increasingly used. The present article describes the measurements aimed at identification of an optimal cooling method and the results of the comparison of surface cooling, circulation cooling, and the combined cooling methods in terms of thermodynamic and energy parameters during hydrogen absorption.

1 Introduction

The use of circulation heating and cooling of MH containers brings certain disadvantages with regard to the heat exchange between the heat-transfer fluid and the surrounding environment, as well as the heat gain from the rotating parts of the pump [1,2]. Thermal capacity produced by the PT is therefore reduced by a considerable portion; this may be eliminated by connecting the PT directly to the shell of the MH container. However, the surface heating (cooling) of containers is accompanied changing the internal heat transfer via the tubular spiral heat exchanger into the surface heating (cooling); this may, due to significantly low thermal conductivity of the powder MH material, prolong the time required for changing the container temperature and increase the pressure during hydrogen absorption as a result of insufficient heat removal [3-7].

2 Characteristics of the measurement stand with a metal hydride container

In order to facilitate the transport of thermal energy between the planar PT attached to the cylindrical surface of the HBond©500 container, it was necessary to construct a heat exchanger (Figure 1) which would also be used for accumulation in order to maintain low temperatures during heat generation in hydrogen absorption.

The surface heat exchanger consists of two mirrored aluminium parts that are screwed together and attached to the surface of the MH container (Figure 2) using the thermally conductive paste on the heat-transfer surfaces in order to reduce the thermal contact resistance.

For the purpose of determination of the difference between the temperatures of the heated side and the cooled side of the PT, temperature sensors T_9 to T_{12} were installed. T_{13} sensor was scanning the ambient temperature which is required for the correct identification of the heat losses and gains from the surrounding environment.

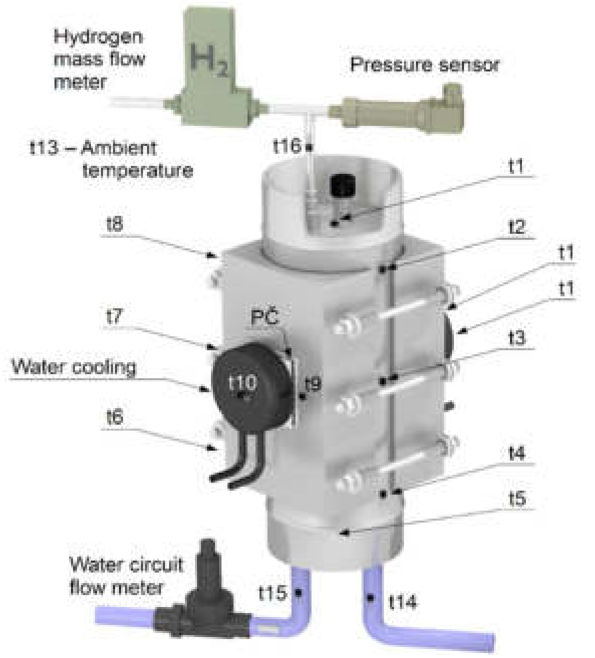

Figure 1 3D model of the MH container with aluminium heat exchanger, PT, water cooling and measuring probes

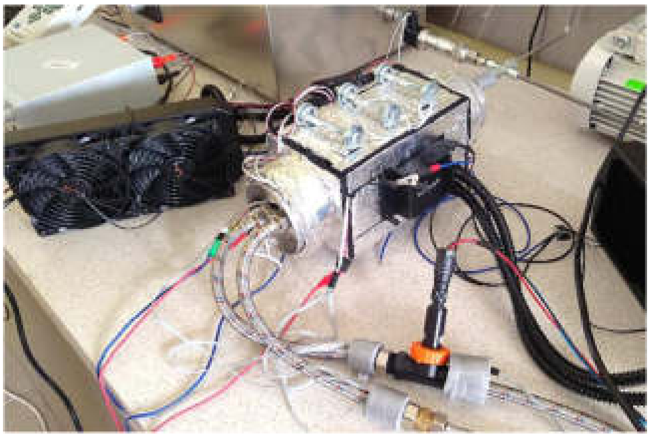

Figure 2 Image of the measurement stand with the MH container

After the sensors were installed, the container was thermally insulated with 10 mm thick foam rubber with the external reflective foil to eliminate the radiant heat flux.

3 Hydrogen absorption into a metal hydride container without cooling

In the first part of the experiment, the measurements were performed with regard to the absorption of 200 litres of hydrogen into a metal hydride container while maintaining the average flow rate of approximately 9.4 $l \cdot min^{-1}$ without cooling. The container was only cooled by free convection from the insulation surface to the surrounding environment.

Hydrogen absorption into the intermetallic structure of the alloy was accompanied with generation of heat that increases the container temperature. Due to the fact that no additional cooling was used, the temperature significantly increased and this also proportionally increased the equilibrium pressure of hydrogen.

The development of the values of the relative pressure and the average container surface temperature, depending on the amount of the absorbed hydrogen, is shown in Figure 3.

Following the absorption of 200 litres of hydrogen into the $La_{0.85}Ce_{0.15}Ni_5$ alloy, weighing 3.125 kg, which lasted 1,270 seconds, the temperature increased in 32.9 °C and the pressure increased in 2.2 MPa. After the hydrogen supply was stopped, the temperature additionally increased due to residual hydrogen absorption.

During hydrogen absorption without cooling, the temperature significantly increased and the pressure increased up to the value close to the permissible maximum limit determined for the HBond©500 container, i.e., 2.5 MPa. It should be noted that the HBond©500 container facilitates storage of maximum 500 litres of hydrogen, so the critical pressure values are usually reached as soon as the container becomes filled in 40 % (at the average hydrogen flow rate of 9.4 $l \cdot min^{-1}$).

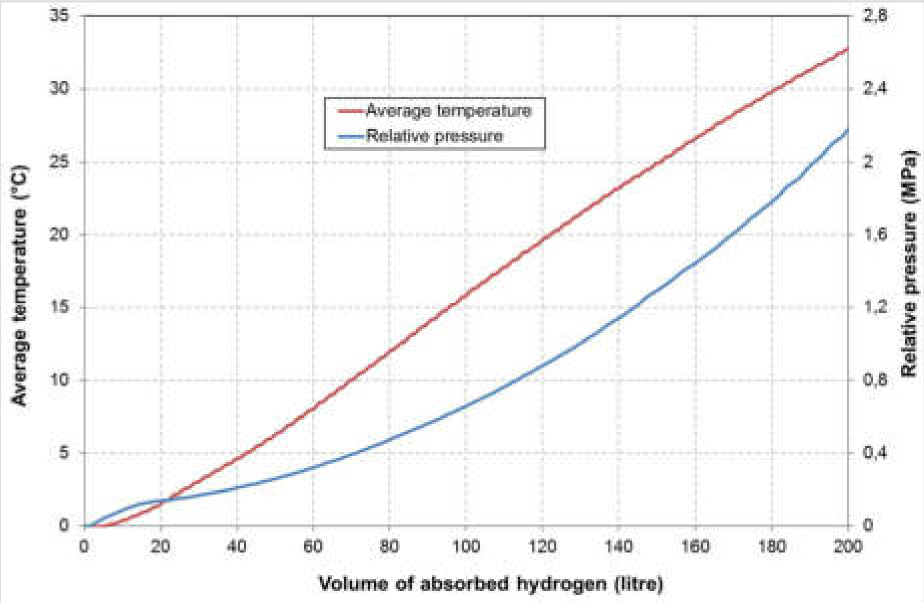

Figure 3 Curves of relative pressures and average container surface temperatures, depending on the amount of the absorbed hydrogen

4 Hydrogen absorption into a metal hydride container with surface cooling

In the second part of the experimental measurements we performed the absorption of 200 litres of hydrogen into an alloy while applying the surface cooling using two PTs arranged as shown in Fig. 1.

The lowest temperature, as to the container surface, was observed on the external cylindrical surface, i.e., at the place where the container is thermally attached to aluminium exchangers. This resulted in the increased concentration of the stored hydrogen, especially in the close vicinity of the external cylindrical surface of the container. However, a disadvantage of the shell cooling is the minimum heat removal from the area along the container axis, as was also indicated by a significant increase in pressure, comparable to the pressure observed when the cooling was not applied. The development of the average surface temperature and the relative pressure of the container, depending on the volume of the absorbed hydrogen, is shown in Figure 4.

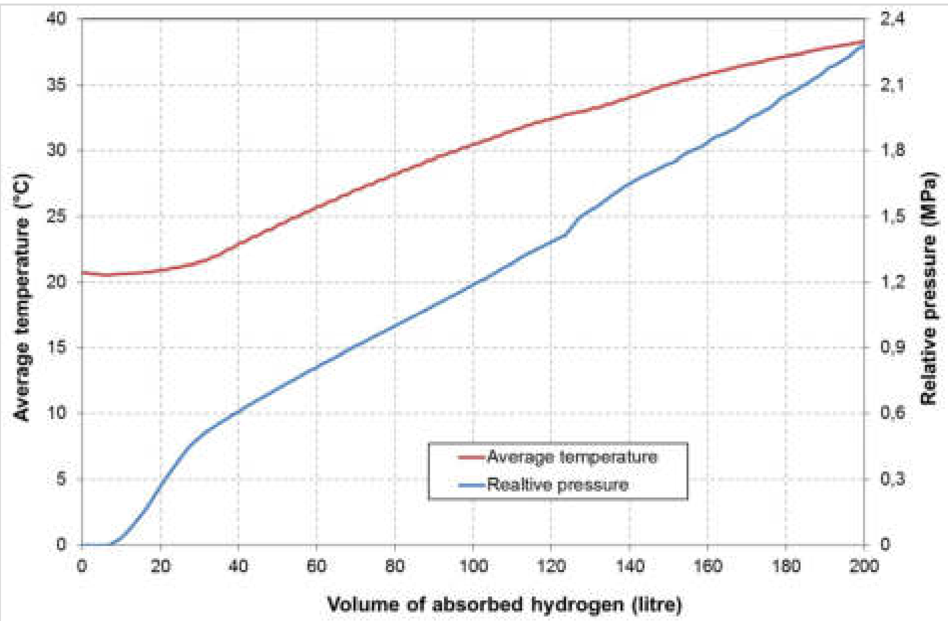

Figure 4 Curves of average surface temperatures and relative pressures of the container, depending on the volume of the absorbed hydrogen

The total increase in the surface temperature, following the absorption of 200 litres of hydrogen, was 17.6 °C; this value was much lower than the one observed during the absorption process without cooling and was primarily caused by the surface cooling without having a more significant impact on the internal thermal field, as indicated by the above mentioned relative pressure in the container.

Figure 5 depicts the development of temperatures on the cold and hot sides of the PT measured by T_9 a T_{10} temperature sensors; the difference between the temperatures was a decisive parameter for the determination of the cooling power, as shown in the graph in Figure 1.

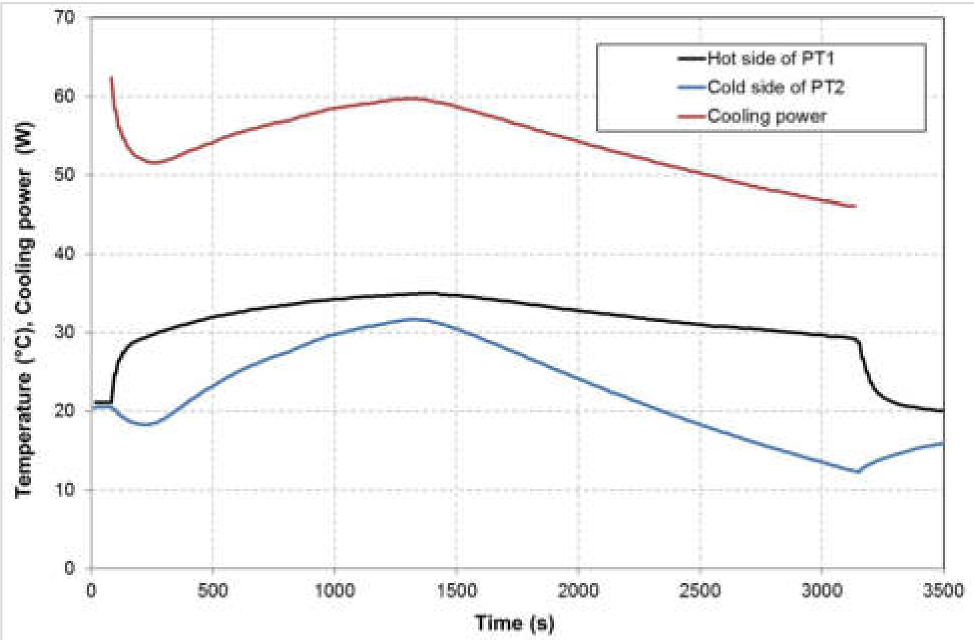

Figure 5 Curves of temperatures on the cold and hot sides of the PT measured by T_9 and T_{10} temperature sensors

The average cooling power of the PT was 108 W (2·54 W); this means that if the average input power is respected, the coefficient of performance of Peltier thermopiles COP cooling is 0.68.

5 Hydrogen absorption into a metal hydride container with the circulation cooling based on the principle of Peltier thermopiles

In the third part of the experimental measurements we performed the absorption of 200 litres of hydrogen into an alloy while applying the circulation cooling using a PT-based cooler.

When compared to the previously applied surface cooling, this cooling method differs in the fact that the water cooled in the external cooler comprising four PTs TEC1-12710 enters the metal hydride container through the inlet of the internal spiral heat exchanger; it is therefore the circulation internal cooling. During the whole period of performing the measurements, the flow rate of the cooling water was 1.18 $l \cdot min^{-1}$ at the maximum performance of the circulation pump. The flow rate value was limited by a small internal diameter of the piping inside the spiral exchanger. The average initial surface temperature of the container was 19.5 °C. Hydrogen absorption began in second 100 and 200 litres of hydrogen were supplied into the container in second 1,400.

The cooling power of the external cooler was identified applying an indirect method, i.e., measurements of the water flow rate, input and output water temperature, with subsequent application of the calorimetric equation.

The maximum cooling power removed from the alloy during hydrogen absorption was 118 W and the internal source of heat generated during the absorption reached the average value of 145 W; this resulted in a gradual increase in the average temperature of the container (Figure 6).

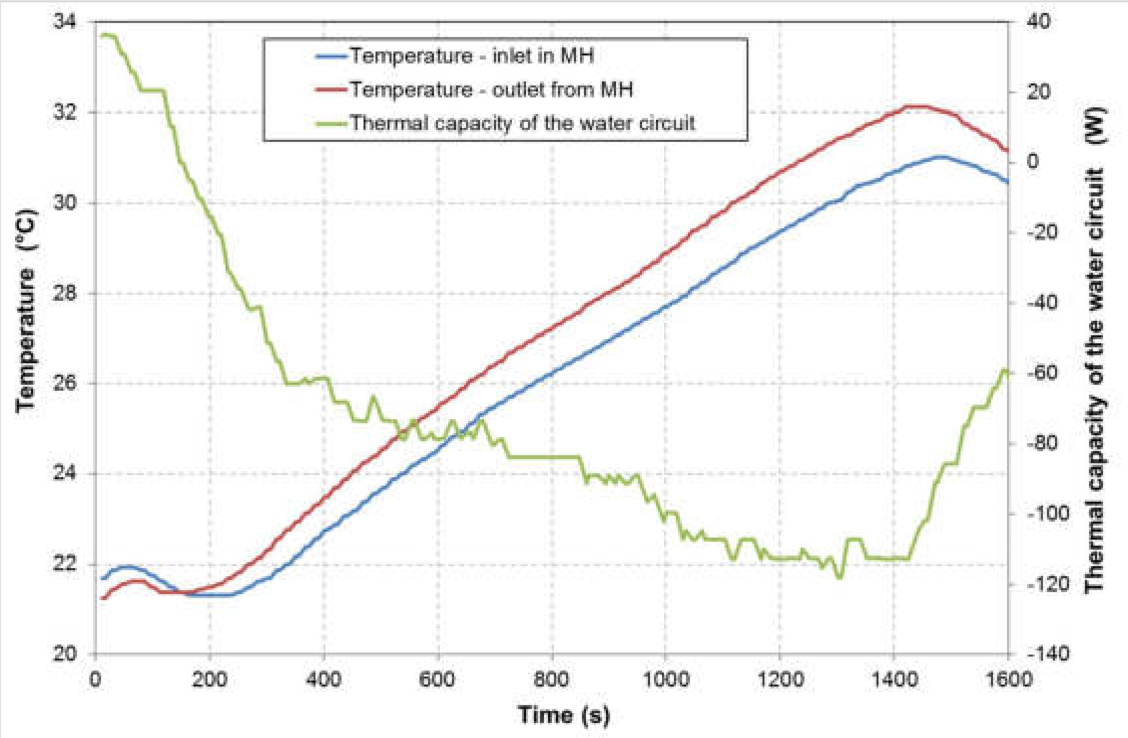

Figure 6 Curves of temperatures and thermal capacities removed by the cooling water

During the absorption of 200 litres of hydrogen into the intermetallic structure with concurrent circulation cooling, the temperature increased in 14.5 °C. With an increasing temperature, the relative pressure of hydrogen increased up to the value of 1.41 MPa (Figure 7).

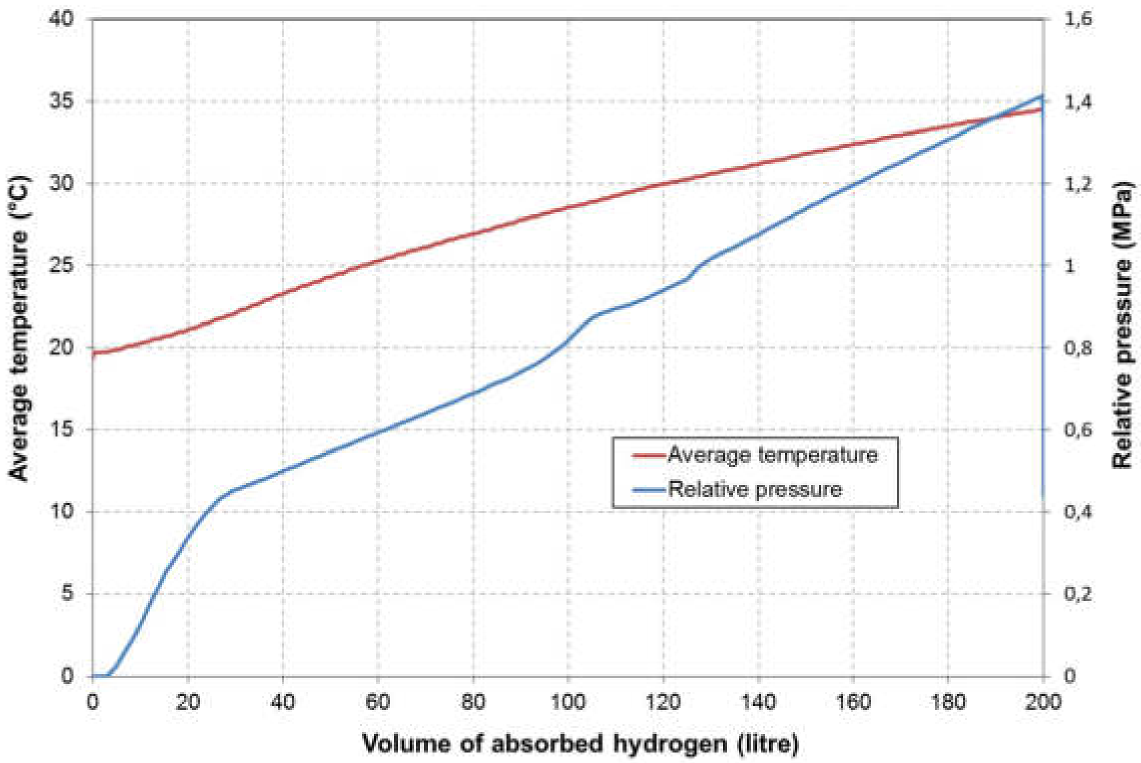

Figure 7 Curves of average temperatures and relative pressures of hydrogen, depending on the volume of the absorbed hydrogen

We may state that when the circulation cooling of the container was applied, the operating parameters of the absorption improved due to the decreased temperature and relative pressure. This was a result of low thermal conductivity of powder metal hydride with which the even distribution of heat-transfer surfaces in the entire volume is more advantageous for heat removal, when compared to the surface cooling. Obviously, increased cooling power was caused by higher performance of four PTs in the circulation cooler, when compared to two PTs applied in the surface cooling.

6 Hydrogen absorption into a metal hydride container with combined circulation and surface cooling methods

In order to point out potential intensification of the cooling effect and subsequent improvement of operating parameters during hydrogen absorption into the alloy, we performed the measurements while combining the surface and circulation methods of cooling the container during hydrogen absorption. During the measurements, the cooling water flow rate was the same as in the previous case, i.e. 1.18 l·min^{-1}.

Temperatures of water at the inlet to and outlet from the MH container and the values of cooling power are shown in Figure 8. The maximum power with the combined cooling was only 85 W.

The equality of the internal heat source and the amount of the heat removed per time unit may also be depicted as the curve of average container surface temperatures, depending on the absorbed quantity of hydrogen (Fig. 9) which was almost constant. With a constant container temperature, we may only expect a minimum increase in pressure with an increasing mass concentration of the absorbed hydrogen. However, the real pressure increase was rather high and at the end of absorption of 200 litres of hydrogen it reached the value of 1.18 MPa.

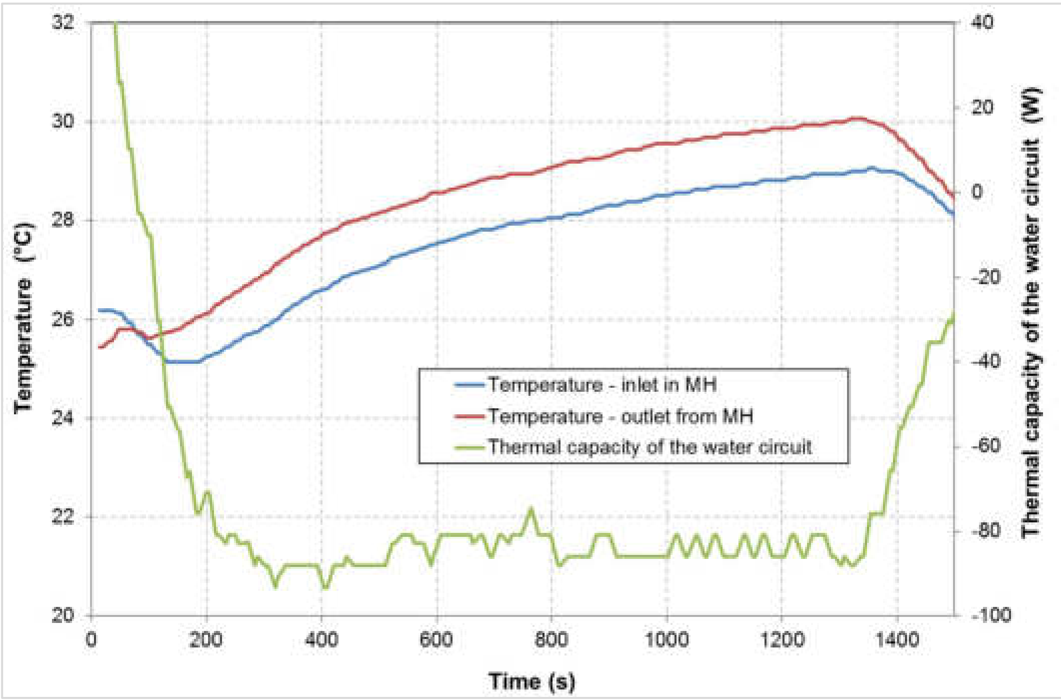

Figure 8 Curves of temperatures and thermal capacities removed by cooling water in the combined cooling of the MH container

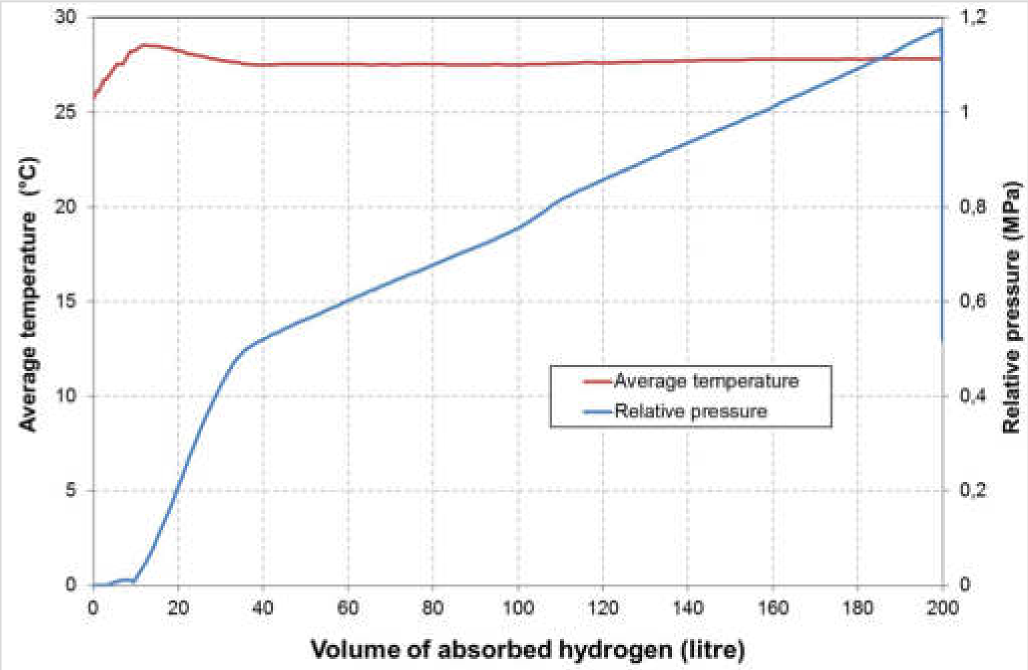

Figure 9 Curves of average temperatures and relative pressures of hydrogen, depending on the volume of the absorbed hydrogen

This was caused by the fact that cooling was concentrated primarily on the surface of the container where the temperature sensors were located; however, along the container axis and at its terminal parts the temperature is expected to rise and, accordingly, the relative pressure would rise too. Nevertheless, the pressure increase was the lowest out of all performed experimental measurements. Moreover, it seems that certain problems may also arise as a result of low thermal capacity of cooling of the circulation heating which is caused by mutual effects of the two independent cooling systems.

7 Conclusion

On the basis of the above described experimental measurements performed in the process of cooling the MH container we may state that due to low thermal conductivity of powder alloys the worst alternative is the surface cooling in which the increases in pressure and temperature observed during hydrogen absorption were the highest.

The circulation cooling resulted in significant pressure decrease. However, there is a potential of optimising the shape of the spiral heat exchanger aimed at increasing the quantity of the heat removed from the terminal parts of the container. The lowest increase in pressure was observed when we combined the surface and the circulation cooling methods; this, however, resulted in a significant increase in the electric energy consumption by the cooling systems.

Chemically bound energy of 200 litres of the stored hydrogen, derived from its combustion heat, was 0.71 kWh. Article shows the energy consumption for individual methods of cooling the MH container, including the percentages of the consumed electric energy required for cooling the container of the total energy contained in hydrogen. The switch from the surface cooling to the circulation cooling resulted in a significant increase in the consumption of energy required for cooling, not to mention the combined method in which the reached values of pressure and temperature were very good, but as much as over 27 % of the stored energy were used for cooling the container.

Acknowledgments
This paper was written with the financial support of the granting agency APPV within the project solution No. APVV-15-0202, of the granting agency VEGA within the project solution No. 1/0108/19 and of the granting agency KEGA within the project solution No. 005TUKE-4/2019

References

[1] BRESTOVIČ, T., JASMINSKÁ, N., ČARNOGURSKÁ, M., LÁZÁR, M.: Measurement and Simulation of Transient Phenomena in Metal Hydride Bed, *Applied Mechanics and Materials*, Vol. 816 (2015), pp. 204-212, 2015.

[2] BRESTOVIČ, T., JASMINSKÁ, N., LÁZÁR, M., KAPUSTOVÁ, Ľ.: Measurement of the operational characteristics of hydrogen storage in a metal-hydride tank, *Journal of Multidisciplinary Engineering Science and Technology*, Vol. 3, No. 9, pp. 5546-5549, 2016.

[3] ANTONYOVÁ, A., ANTONY, P., KORJENIC, A.: Laboratory measurement of thermal distribution throughout the insulation materials using the Peltier module while managing elimination of external influences, *Article Energy and Buildings*, Vol. 128 (2016), pp. 336-348, 2016.

[4] GONCALVES, L.M., ROCHA, J.G., COUTO, C., ALPUIM, P., CORREIA, J.H.: On-chip array of thermoelectric Peltier microcoolers, *Article Sensors and Actuators A: Physical*, Vol. 145-146, No. July-August, pp. 75-80, 2008.

[5] GRENIER, CH., KOLLATH, C., GEORGES, A.: Thermoelectric transport and Peltier cooling of cold atomic gases Comptes, *Rendus Physique*, Vol. 17, No. 10, pp. 1161-1174, 2016.

[6] HERMES, CH.J.L., BARBOS, J. R.: Thermodynamic comparison of Peltier, Stirling, and vapor compression portable coolers, *Article Applied Energy*, Vol. 91, No. 1, pp. 51-58, 2012.

[7] KANG, B.H., PARK, C.W., LEE, C.S.: Dynamic behaviour of heat and hydrogen transfer in a metal hydride cooling system, *International Journal of Hydrogen Energy,* Vol. 21, No. 9, pp. 769-774, 1996.

Review process

Single-blind peer review process.

doi:10.22306/atec.v5i4.58

Received: 26 June 2019
Accepted: 08 Nov. 2019

OPERATION OF THE AUTOMATIC HEAT SOURCE ON PELLETS WITH VARIOUS BURNER TYPES

Michal Holubčík
Department of Power Engineering, University of Žilina, Univerzitná 1, 010 26 Žilina, Slovak Republic, EU, michal.holubcik@fstroj.uniza.sk (corresponding author)
Nikola Kantová
Department of Power Engineering, University of Žilina, Univerzitná 1, 010 26 Žilina, Slovak Republic, EU, nikola.kantova@fstroj.uniza.sk
Juraj Trnka
Department of Power Engineering, University of Žilina, Univerzitná 1, 010 26 Žilina, Slovak Republic, EU, juraj.trnka@fstroj.uniza.sk
Jozef Jandačka
Department of Power Engineering, University of Žilina, Univerzitná 1, 010 26 Žilina, Slovak Republic, EU, jozef.jandacka@fstroj.uniza.sk

Keywords: heat source, wood pellets, burner, biomass, boiler

Abstract: One of the most important issues in choosing a heating system is the question: What kind of fuel can be burned in given heating system. Modern automatic solid fuel boilers are often specialized only on a narrow range of suitable pellet materials. Pellets from cheaper sources are also beginning to appear on the market. However, many burners are unable to burn these new types of pellets without significant burning problems. The article deals with the influence of the proper construction of the burner on the smoothness of the combustion process and the smooth operation of the combustion equipment. The results of the experiments document the continuity of the combustion plant in the combustion of less quality pellets containing bark using more modern combustion technologies. In fact, less quality pellets cause the formation of ash sinters which cause the continuous combustion process to be interrupted, resulting in fluctuations in equipment performance and the onset of thermal discomfort. The results showed no problem with burning even when making sinters, but also showed a fluctuation in performance and the need for manual control, especially when heating or clogging the supply pipe. They also showed significant damage to pellets in the worm feeder section. These problems, therefore, ultimately require further research to ensure complete, seamless operation.

1 Introduction

1.1 Solid fuels

Automatic small heat sources for solid fuels most frequently use wood pellets as fuel. Pellets are small granulated cylinders of circular cross-section with a diameter of 2.5 to 8 mm with a length of up to 5 cm [1,2]. Their unquestionable advantage is their normalized size, which allows us to continuously run the combustion and control the output of the combustion equipment as needed. In addition, we can use different types of materials to produce new types of fuel. However, this trend also brings with it some problems. The use of less quality biomass for combustion, changes the chemical composition of the fuel and, in particular, the ash content of the substances. These substances in plant fitness have been shown to have an effect on reducing the melting point of ash. The problem of plant ash is free oxides (and chlorides) which significantly reduce the value of the melting point of ash. Silicon dioxide plays an essential role in vitreous oxide and calcium oxide together with potassium oxide subsequently reduces the viscosity of the resulting melt [3,4]. The first is that they form meteor-like crystals that, due to their higher weight, remain in the burner and clog it and prevent new fuel from entering the burning process. They also settle on the burner walls and cause a reduction in the combustion space cross section [5]. The burner burners are particularly susceptible. The article deals with the appropriate design of the burner with respect to the mentioned problem.

1.2 Influence of flame direction

One of the most striking effects of combustion is the flame direction. In practice, it is possible to burn solid fuels in only two ways, either horizontally or vertically, or alternatively by combining these two methods. From our point of view, one of the most important factors in combustion is gravity, which acts on the unburned pellets as well as on the burnt residue of the ash. The ash itself will not become such a problem because small ash particles with their weight are easily blown out of the torch body [6,7]. The problem arises when sintering because the ash gains weight and the larger the sinter is, the greater the gravitational force acting on it. For this reason, vertical retort burners are unsuitable for incineration of lower quality biomass because the resulting sinters must go out directly against the gravitational force [8,9]. In tubular horizontal burners, the situation is much better as the sinters no longer have to overcome the gravitational but only frictional force on the tube wall and are mostly blown out of the burning process without problems. NO disadvantage of this system is that even unburned pieces of pellets can easily fall out of the burning process [10,11]. Some compromise is to tilt the burner upwards, at an angle at which the pellets would remain in the tube and burn smoothly. Otherwise, with extremely high sintering, the burner can be tilted down in the direction of gravity to prevent burner clogging. In our experiment, we compared the results of both systems as shown in figure 1.

Figure 1 Flame direction – retort burner on the left, tube rotary burner on the right

2 Materials and methods

2.1 Used fuel samples

Spruce wood with different bark content was used as fuel (figure 2):

- sample 1 (V1) - 100% bark-free spruce wood pellets,
- sample 2 (V2) - 95% spruce wood pellets with bark content 5%,
- sample 3 (V3) - 90% spruce wood pellets with 10% bark,
- sample 4 (V4) - 80% spruce wood pellets with a bark content of 20%.

Prior to measurement, the moisture content of the individual samples was determined on a RADWAG 50 SX drying scale and calorific value using a LECO AC 500 calorimeter.

Figure 2 Wood pellets samples

2.2 Methods of experiments

The combustion took place in commercial small heat source USPOR 18 AUTOMAT with a rated heat output of 18 kW which was tested on an experimental device designed for the measuring of heat output and emission production. The connection of an automatic heat source to the experimental device can be seen in figure 3. The device is built from an experimental boiler, a heat consumption device (i.e. device for regulation of heat produced by the boiler), a gaseous emission analyser, a particulate matter analyser, measuring apparatus to which all measuring instruments are connected and a computer for the processing of measured data. Various parameters are recorded every 20 s. During the measurements constant chimney draft 12 ± 2 Pa via a flue fan is ensured. Its speed is controlled by a frequency regulator.

Experimental measurements to determine the effect of the burner design on the combustion process were performed on a local heat source with a maximum power of 18 KW, where two types of burners were mounted. First, measurements were made with the original retort burner compatible with the source. Second measurements were made after replacing the retort burner with a newer type of rotary burner for which the combustion equipment had to be adapted. All pellet samples with various bark content were burned at the same operating settings of the boiler – fuel feeding time of a spiral conveyor is 18 s, idle time of the conveyor is 25 s, the combustion air is set to constant air access. This operation mode correspond with the loading process in other works [11,12]. The boiler was operated on settings for nominal heat output during wood pellets with very good quality burning.

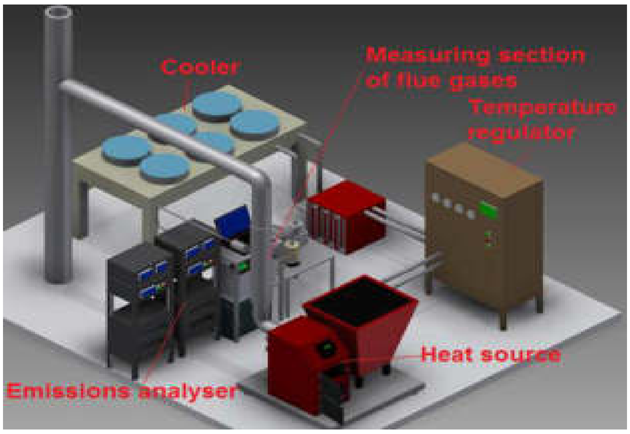

Figure 3 Experimental device for heat source testing

The thermal power of an experimental boiler was measured by calorimetric method where the flow of the heat transfer medium (water) was measured by a magnetic flow meter YOKOGAWA ADMAG AXF with an accuracy of ±0.35 %. The temperature difference of the heat transfer medium (water) was measured by two paired resistance thermometers PT100 with a measurement accuracy ±0.4 %.

Acta Tecnología - International Scientific Journal about Technologies
Volume: 5 2019 Issue: 4 Pages: 81-85 ISSN 2453-675X

The concentrations of O_2, CO_2, CO, NO_x in flue gases were measured by a flue gas analyser ABB AO 2020 with sensor modules Uras 26 (NDIR photometer for continuous CO_2, CO, NO_x measuring) with accuracy ≤ 1 % of span and oxygen analyser module Magnos 206 (paramagnetic behaviour of oxygen) with accuracy ± 0.5%. The suction pyrometer is used for sampling exhaust gas. Pyrometer output socket connects to the flue gas analyser. The piping for the sampling operations must be incorporated with means for cooling, cleaning and drying flue gas samples. ABB analyser AO 2020 is constructed according to the requirements and nature of the measurement. Recorded the emission values in ppm units (parts per million). These values were converted to $mg.m^{-3}$. The normalized concentration of oxygen in the flue gas from a boiler O_{2n} is 10 %. Therefore, the measured values of each emission are recalculated.

Particulate matter measurement was conducted by gravimetric method by using of the isokinetic automatic sampler TECORA Isostack Basic. Gravimetric method is given by the standard ISO 9096 [9,10]. It is a manual, single-use method where samples are taken by a probe from flowing gas. This method gives an average value of PM for a given span of time within which a partial flow from an exhaust gas sample is taken. Exhaust gases are guided through filtration or sediment systems which catch either all particles or only those of pre-defined size. Filtration materials are weighed before and after measurements and final mass concentration is calculated from a sample volume. Sampling probes can be placed either directly into hot flow of exhaust gases or outside the flow (these systems must be heated to avoid condensation or nucleation). Solid particles are collected from flowing gas with the help of the probe. From them an average concentration of flowing gas particles is determined. Exhaust gases were taken from a chimney duct with the help of a three-stage separation impactor. The sampling was conducted at the same speed of exhaust gas flow as in the pipe. Hot gas was led from the pipe through cooling and drying equipment up to the sampling unit. In the cooling equipment exhaust gases were cooled and water vapour was removed from the exhaust gas sample. In the silica gel-water absorption tower residual moisture of exhaust gases was removed. The accuracy of this method influences various parameters, mainly differential pressure in Pitot tube ± 4 Pa, temperature of flue gas ± 0.7 %, flow rate and volume measure ± 2 % and filter weight ± 0.1 mg. The sampling was isokinetic and the isokinetic deviation during all experiments was in the range -5.7 ÷ 4.9 %.

3 Results

The measurement values compare the combustion of four identical sample types in two different types of combustion burners. Table 1 shows the average measured values of the determined parameters during the experiments on retort burner.

Table 1 Average measured values of the determined parameters during the experiments on retort burner

	V1	V2	V3	V4
Thermal power (kW)	13.2	15	14.6	14.4
Efficiency (%)	75.3	76.4	75.7	75.7
O_2 (%)	14.1	13.1	13.1	13
CO_2 (%)	6.8	7.6	7.6	7.7
$CO_{10\%}$ ($mg.m^{-3}$)	1381.8	929.2	771.9	703.4
$NO_{X10\%}$ ($mg.m^{-3}$)	232.6	254.5	243.9	271.6
$OGC_{10\%}$ ($mg.m^{-3}$)	20.1	21.4	32.6	29.8
$PM_{10\%}$ ($mg.m^{-3}$)	25.4	29.5	35.3	41.1

Table 2 shows the average measured values of the determined parameters during the experiments on rotary tube burner.

Table 2 Average measured values of the determined parameters during the experiments on rotary burner

	V1	V2	V3	V4
Thermal power (kW)	14.6	17.8	17.9	18.2
Efficiency (%)	87.6	90.4	90.9	90.6
O_2 (%)	12.2	6.4	5.4	7.5
CO_2 (%)	8	14.3	15.4	13.4
$CO_{10\%}$ ($mg.m^{-3}$)	795.8	1598.1	2718.5	3613.7
$NO_{X10\%}$ ($mg.m^{-3}$)	228.6	177.1	149.1	199.9
$OGC_{10\%}$ ($mg.m^{-3}$)	30.3	13.3	84.4	69.7
$PM_{10\%}$ ($mg.m^{-3}$)	35.6	46.4	48.5	57.7

It is clear from the measured values that when using a rotary burner, the efficiency of the conventional type of retort burner was increased by almost 15%. Increasing combustion efficiency has led to a reduction in the chimney temperature and temperature in the combustion chamber, which has been positively reflected in a decrease in NO_X emissions. Also, the bark used has had a positive effect on the fire turbulence, which has led to an increase in plant performance.

Figure 4 shows time course of thermal power of heat source with various burners. Retort burner had more stable operation which cause almost constant thermal power. On the other hand, the operation of tube burner was not so stable, but the combustion efficiency was higher.

A major disadvantage of tube burning using was the excessively high emission production of CO caused by the dropping of the unburned parts of the pellets from the burner compartment which is into the ashtray what is shown on figure 5. Despite this the average CO production during tube rotary burner using is half in comparison with boiler operation with retort burner.

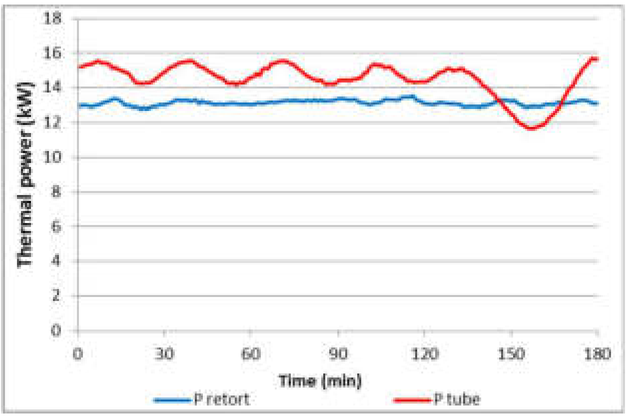

Figure 4 Time course of thermal power of heat source with various burners

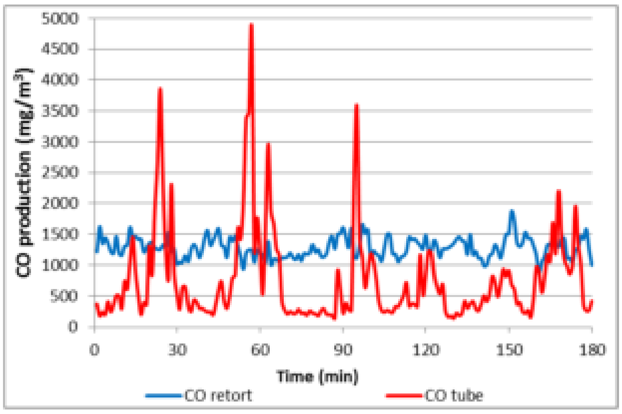

Figure 5 Time course of CO production of heat source with various burners

4 Conclusion

Research has shown that the burning direction and slope of the burner significantly affect the efficiency and smooth operation of the combustion plant. More modern horizontal burner types do not have to overcome the gravitational force that acts on the ash and the resulting sintering prevents these particles from blowing out of the burner combustion chamber and causes the combustion chamber to clog. On the other hand, the reduced effect of the gravitational force on the non-burnt fuel causes the still unburdened pellets to be blown into the burner into the combustion chamber where these pellets do not fully heat up or imperfectly without optimum air and temperature access. This leads to an increase in mechanical and chemical loss, and in particular an increase in CO emissions. A suitable compromise is the use of a rotary burner with a suitable tilt angle, which would increase the gravitational force required to blow the unburnt particles from the burner.

Acknowledgement

This article was supported by the projects KEGA 033ŽU-4/2018 "Heat sources and pollution of the environment", APVV-15-0790 "Optimalization of biomass combustion with low ash melting temperature" and VEGA 1/0233/19 "Construction modification of the burner for combustion of solid fuels in small heat sources".

References

[1] JANDAČKA, J., MIČIETA, J., HOLUBČÍK, M., NOSEK, R.: *Innovation to make the biomass combustion process more efficient*, Žilina, EDIS, pp. 265, 2016. (Original in Slovak)

[2] MIKULOVA, Z., VITAZEK, I.: *Proportion of volatile matter in selected biofuels*, Proceedings of International PHD Students Conference, (Mendelnet 2016), pp. 892-897, 2016.

[3] BRESTOVIČ, T., JASMINSKA, N.: Software support development for numerical solution of ansys CFX, *Acta Mechanica et Automatica,* Vol. 7, No. 4, pp. 215-221, 2013.

[4] DZURENDA, L., HRONCOVÁ, E., LADOMERSKÝ, J.: Extensive Operating Expe-riments on the Conversion of Fuel-Bound Nitrogen into Nitrogen Oxides in the Combustion of Wood Fuel, *Forests*, Vol. 8, No. 1, pp. 1-9, 2017.

[5] WEBER, R., SZLEK, A., NOSEK, R.: Time-dependent combustion of solid fuels in a fixed-bed: measurements and mathematical modeling, *Energy & fuels*, Vol. 28, No. 8, pp. 4767-4774, 2013.

[6] CHUDÍKOVÁ, P., TAUŠOVA, M., ERDELYIOVA, K,. TAUŠ, P.: Potential of dendromass in Slovak Republic and its actual exploitationin thermic economy, *Acta Montanistica Slovaca*, Vol. 15, No. 2, pp. 139-145, 2010.

[7] DZURENDA, L., BANSKI, A.: Dependence of the boiler flue gas losses on humidity of woody biomass, *Archives of Thermodynamics*, Vol. 36, No. 4, pp. 77-86, 2015.

[8] RIMÁR, M., FEDÁK, M., KORSHUNOV, A., KULIKOV, A., MIŽÁKOVÁ, J.: Determination of Excess Air Ratio During combustion of Wood Chips Respect to Moisture Content, *Acta Facultatis Xylologiae*, Vol. 58, No. 2, pp. 133-140, 2016.

[9] HORAK, J., KUBONOVA, L., KRPEC, K., HOPAN, F., KUBESA, P., MOTYKA, O., LACIOK, V., DEJ, M., OCHODEK, T., PLACHA, D.: PAH Emissions from Old and New Types of Domestic Hot Water Boilers, *Environmental Pollution*, Vol. 225, pp. 31-39, 2017.

[10] HONUS, S., POSPÍŠILÍK, V., JURSOVÁ, S., ŠMÍDA, Z., MOLNÁR, V., DOVICA, M.: Verifying the Prediction Result Reliability Using k-ε, Eddy Dissipation, and Discrete Transfer Models Applied on Methane Combustion Using a Prototype Low-Pressure Burner, *Advances in science and technology-research journal*, Vol. 11, No. 4, pp. 252-259, 2017.

[11] ESKILSSON, D., RÖNNBÄCK, M., SAMUELSSON, J., TULLIN, C..: Optimisation of efficiency and emissions in pellet burners, *Biomass and Bioenergy*, Vol. 27, No. 6, pp. 541-546, 2004.

[12] DIAS, J., COSTA, M., AZEVEDO, J.L.T.: Test of a small domestic boiler using different pellets, *Biomass and Bioenergy*, Vol. 27, No. 6, pp. 531-539, 2004.

Review process

Single-blind peer review process.

Acta Tecnología - International Scientific Journal about Technologies
Volume: 5 2019 Issue: 4 Pages: 87-92 ISSN 2453-675X

doi:10.22306/atec.v5i4.59
Received: 26 June 2019
Accepted: 09 Nov. 2019

PERFORMANCE POTENTIAL OF HEAT PUMP DRYING CYCLES

Bystrík Červenka
Department of Power Engineering, University of Žilina, Univerzitná 1, 010 26 Žilina, Slovak Republic, EU, bystrik.cervenka@fstroj.uniza.sk (corresponding author)
Michal Holubčík
Department of Power Engineering, University of Žilina, Univerzitná 1, 010 26 Žilina, Slovak Republic, EU, michal.holubcik@fstroj.uniza.sk
Milan Malcho
Department of Power Engineering, University of Žilina, Univerzitná 1, 010 26 Žilina, Slovak Republic, EU, milan.malcho@fstroj.uniza.sk
Nikola Kantová
Department of Power Engineering, University of Žilina, Univerzitná 1, 010 26 Žilina, Slovak Republic, EU, nikola.kantova@fstroj.uniza.sk

Keywords: heat pump, drying, drying rate, energy efficiency
Abstract: There are two thermodynamic models of the closed and vented heat pump drying process described in the paper. The models have been used for optimization of process design parameters with respect to drying rate and energy efficiency, respectively. The optimization was performed in points of parametric space defined by refrigerant and air flow rates. Results of the optimization shows the same maximal drying rate performance for closed cycle and both objective functions. There is higher potential of drying time reduction for vented cycle in comparison to closed cycle. Results of the optimization showed strong correlation of the MER parameter with refrigerant flow rate for both closed and vented heat pump drying cycle. There is same maximal MER value obtained for both MER and SMER optimized cycle parameters.

1 Introduction

There are numerous reports which identified the drying operation as very energy intensive and demanding process, Minea [1]. In contrast to drying energy consumption a minimal requirement on drying rate are posed by industry users and end consumers on the process, though.

There are numerous ways how to remove water from a material, to be dried out, which were adopted in various industrial applications. A lot of processes utilize humidification and dehumidification of air for drying – so called hot-air drying.

Number of scientist and researchers have tried to improve drying rate and energy effectiveness of the different drying process. The studies analysed different drying cycles, their component arrangement or effect of different cycle parameters on their performance. Conde [2] pointed out that the heat pump is suitable device for heat recovery in drying process. He further proposed two system with heat recovery heat exchanger as the heat pump was concluded to represent high capital costs. Lambert [3] developed a model for partially vented drying process and concluded that optimal air recirculation ratio should be on level of 75%.

Several measures for energy savings were experimentally analysed by Hekmat [4]. The study reported e.g. 10-18% of energy saving by 67% of air recirculated. The highest, 33% of energy saving was achieved by test with heat pump. Though, the drying time should have been very long. Bansal [5] compared performance of different closed and vented drying cycles employing condensing and heat recovery heat exchangers, based on thermodynamic model. The highest energy savings of 14% was predicted for closed system with condensing heat exchanger and heat recovery compared to basic vented cycle.

Performance of several, pure heat pump dryer configurations, with focus on tropical climate conditions, were studied by Saensabai [6,7]. He reported different best operating configuration with respect to high and low drying rate period and ambient temperature level.

Any drying process, which operates in closed air cycle, is connected to heating and cooling of the process air. HP drying represents very energy efficient way of air dehumidification as it incorporates heating and cooling of air in regenerative way. Among the couple of HPs technologies, the vapor compression process became accessible in wide range of power output scales.

Air dehumidification takes place in evaporator, at low HP temperature level when the air is cooled below its dew point [8,9]. The drying potential of air is recovered by its successive heating in condenser. The heat extracted from air in evaporator can be regarded as heat regenerated from low temperature air for its re-use at high temperature in condenser.

The performance of HP drying process can be influenced by the HP cycle configuration and controlled by selected low and high temperature levels – evaporator and condenser pressures.

The objective of the study is to examine two HP configuration and their drying potentials in terms of energy consumption and drying time.

2 Thermodynamic model

The two configurations described in the paper are represented by closed (Figure 1) and vented (Figure 2) HP dryer. The drying performance of the HP dryer is investigated numerically making use of thermodynamic model.

The HP dryer is represented by steady state model, which is usually employed to simulate constant drying rate period. The period is important in terms of drying performance as the drying rate attains the highest level during the period. The drying process designer thus usually intents to promote the period within the whole drying cycle.

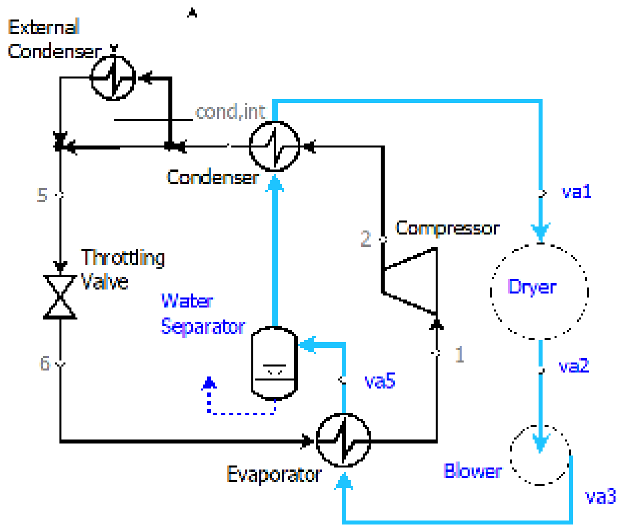

Figure 1 Closed HP dryer components configuration

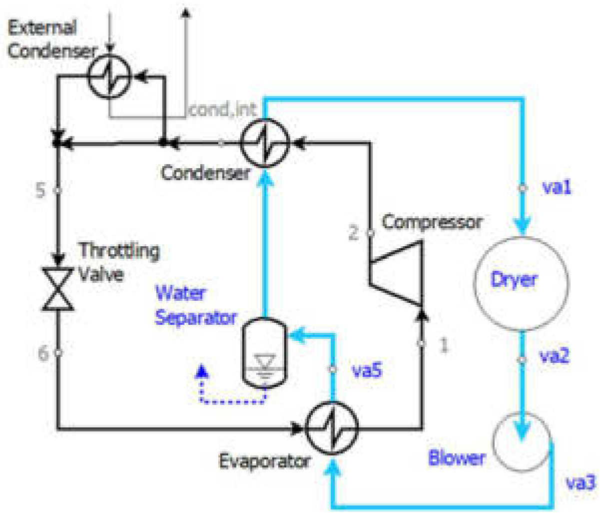

Figure 2 Vented HP dryer components configuration

Following assumptions are summarized as they are applied within the drying model:

- Constant drying rate.
- No pressure drops in refrigerant circuit piping → constant evaporation, condensation pressure.
- Isenthalpic expansion process in throttling device.
- Constant refrigerant superheating in evaporator and subcooling in condenser.
- Negligible heat loss in refrigerant piping and air ducts.
- Constant static pressure in dryer.
- Pinch point temperature difference between refrigerant and air stream in condenser and evaporator.
- Constant power input for auxiliary drives and constant fan efficiency.

The refrigeration cycle is fully defined by evaporation and condensing pressures; p_E, p_C, superheating and subcooling temperature differences; d_{tsh}, d_{tsc} and compressor performance, Figure 3.

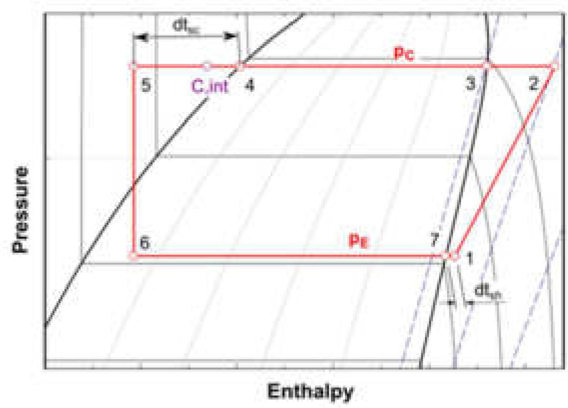

Figure 3 Refrigerant air cycles

2.1 Compressor model

The compressor isentropic and volumetric efficiency model is correlated to measured compressor data according to model described by Carrington [7]. The model is based on six constant polynomials, which relates suction pressure and logarithm of pressure ratio to isentropic and volumetric efficiency parameters.

The model is represented by set of conservation equations for mass of dry air, water/vapor and energy. The equations are constructed for each component in the drying cycle and solved simultaneously, Figure 4.

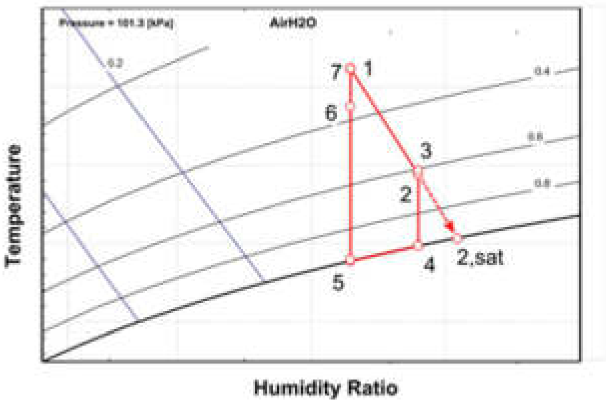

Figure 4 Process air cycles

There is the same mass flow rate in and out of dry air assumed in each of the component. The dry air mass conservation reduces to following equation (1) for each of the component:

$$\dot{m}_{a,in} = \dot{m}_{a,out} = \dot{m}_a \qquad (1)$$

2.2 Dryer model

Conservation of water flow rate in the dryer accounts for water removed from load. The energy accounts for heat loss from the dryer. The constant drying rate assumption is represented by dryer saturation effectiveness parameter, DE.

2.3 Evaporator model

Conservation of water in evaporator takes into account condensed water flow rate from humid air out of the cycle.

2.4 Condenser model

There is no water removed nor added to the air stream in the condenser. The energy equation takes into account energy transfer from refrigerant to drying air.

In contrast to the vented cycle, there is only part of condenser heat transfer from refrigerant to air stream in closed cycle. The part of the heat is referred to as internal condenser; $Q_{\_(C,int)}$. It is necessary to remove some heat out of the system in order to keep it in thermal equilibrium. There is auxiliary condenser and corresponding heat; $Q_{\_(C,aux)}$ used in the model for this purpose (Table 1).

Table 1 Summary of closed cycle conservation equations

Component	Quantity	Equations
Dryer	*Water* *Energy*	$\dot{m}_a\omega_1 + \dot{m}_{wD} = \dot{m}_a\omega_2$ $\dot{m}_a h_{va,1} = \dot{m}_a h_{va,2} + Q_{D,loss}$
	Dryer effectiveness	$DE = \omega_2 - \omega_1/\omega_{2,sat} - \omega_1$
Evaporator	*Water* *Energy*	$\dot{m}_a\omega_3 = \dot{m}_a\omega_5 + \dot{m}_{cw}$ $\dot{m}_a h_{va,3} = \dot{m}_a h_{va,5} + Q_E$
Condenser	*Energy*	$\dot{m}_a h_{va,6} + Q_{C,int} = \dot{m}_a h_{va,8}$
Blower	*Energy*	$\dot{m}_a h_{va,2} + P_B = \dot{m}_a h_{va,3}$

Energy balance in the condenser and evaporator is applied assuming minimal approach (pinch) temperature difference; dt_p, between air and refrigerant streams. Example of temperature profile in idealized counterflow condenser and evaporator could be seen in the Figure 5.

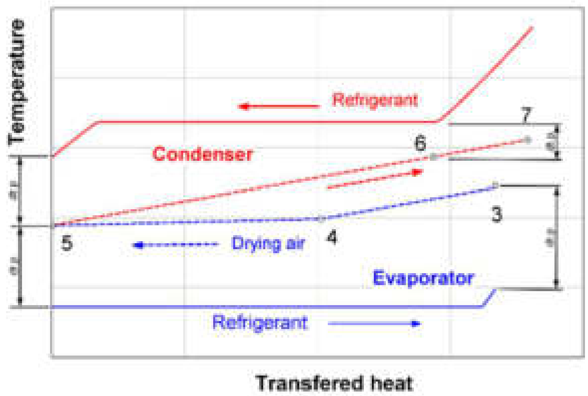

Figure 5 Temperature - duty curve in evaporator and condenser

The two components are treated the same way. There is only energy added to the air stream without affecting water content in dry air. The electric heater is usually not used during the constant drying rate period in order to save energy used for drying.

3 Parametric study with optimized cycle parameters

The performance of the drying cycles is assessed in terms of drying rate and energy consumption for drying of load. Following definitions are adopted for the two parameters: moisture extraction rate (2) and specific moisture extraction rate (3).

$$MER = \dot{m}_{wD} \qquad (2)$$

$$SMER = \frac{\dot{m}_{wD}}{P_{tot}} \qquad (3)$$

Parametric studies have been performed for both of the HP dryer cycle configurations. The refrigerant and air mass

Acta Tecnología - International Scientific Journal about Technologies
Volume: 5 2019 Issue: 4 Pages: 87-92 ISSN 2453-675X

flow rate have been selected as independent parameters for closed cycle. As the refrigerant and air mass flow rates are dependent for the vented cycle, the refrigerant mass flow rate has been used as the only independent parameter for the cycle.

A genetic algorithm approach has been used to optimize design parameters within each discrete point of parametric space. The MER and SMER parameter have been used as respective objective functions for the optimization. Optimization parameter settings with additional constraints are summarized in the Table 2 for both cycle configurations.

Table 2 Optimization parameters selection

Parameters				
Cycle	Independent	Design	Constant	Constraints
Closed	m_r, m_a	p_E, dt_{sc}	p_C, dt_{sh}, DE	$dt_p \geq dt_{p,lim}$
Vented	m_r	p_E, p_C, dt_{sc}	dt_{sh}, DE	$V_a \leq V_{a,lim}$

The optimization of the design parameters for both cycles is subjected to constrained value of a minimal pinch point temperature difference and a maximal volumetric air flow rate.

4 Results and discussion

4.1 Closed cycle

Performance of MER and SMER optimized closed cycle in parametric space is shown on contour plot in the Figure 6 and in the Figure 7. The MER and SMER performance is normalized to a reference value and shown in normalize coordinate space of parametric variables with contour plot of optimal evaporator pressure.

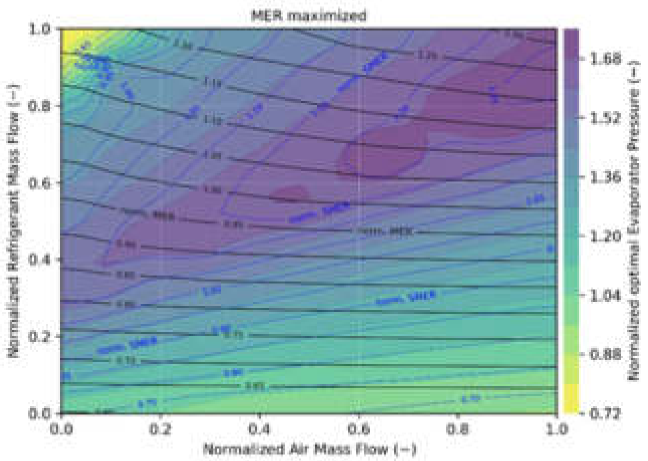

Figure 6 Optimal performance of close cycle for MER objective function

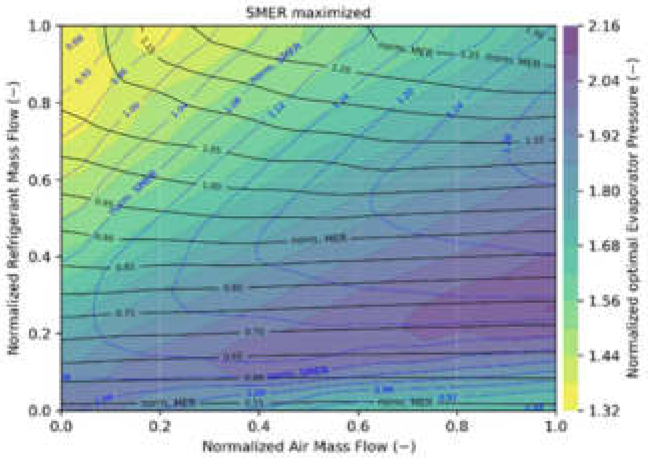

Figure 7 Optimal performance of close cycle for SMER objective function

The results show that there is higher optimal evaporator pressure computed for SMER maximized cycle in comparison to MER optimization. Interestingly, the optimal evaporator pressure is not the lowest possible value from the optimization range. The fact could be explained by increased specific evaporation heat exchanged with increased evaporator pressure.

In both cases there is strong variation of MER parameter with refrigerant mass flow and relatively low dependence on air mass flow rate. Contrary to this, there is stronger dependence of SMER parameter on air mass flow rate, which attain local maximum for a particular value air flow rate.

The contour lines of SMER parameter strongly correlates with optimal value of evaporator pressure for MER optimized cycle. There is no such correlation in case of SMER optimized results.

Both, maximal value of MER parameter and it location in parametric space are almost identical for MER and SMER maximized cycles. The region of the maximal MER value is located in high-high point of refrigerant and air mass flow rate parametric space. Contour plots of SMER parameter show, that there is no more than 2% compromised maximal SMER value for MER maximized cycle. The locus of maximal SMER values, for particular air flow rate, is slightly shifted towards lower refrigerant mass flow rate for SMER maximized cycle.

4.2 Vented cycle

Results of the vented cycle optimization are shown in the Figure 8 for MER and in the Figure 9 for SMER objective functions. There is almost linear variation of MER parameter on refrigerant flow rate in most of its range for both MER and SMER maximization. The maximal value of MER parameter achieved is about 6% higher for MER maximization compare to SMER maximization.

The natural selection of operating point for MER maximized cycle is in higher refrigerant flow rate, as both MER and SMER parameter attain its maximal value in the

Acta Tecnología - International Scientific Journal about Technologies
Volume: 5 2019 Issue: 4 Pages: 87-92 ISSN 2453-675X

range. Contrary to this, either MER or SMER performance parameter is compromised in case of selection of operating point for vented cycle according to the SMER maximized results. Indeed, the two parameters attain its maximal value on different parts or refrigerant flow range. The maximal value of SMER for SMER maximized configuration is about 22% higher and obtained for refrigerant flow rate in its lower range, in comparison to MER maximized configuration.

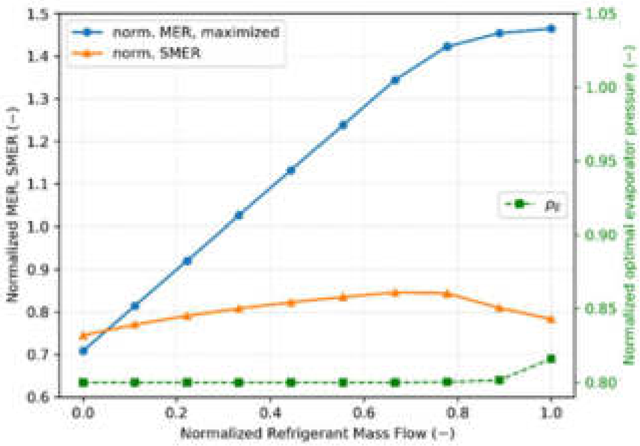

Figure 8 Optimal performance of vented cycle for MER objective function

The flat variation of optimal evaporator pressure for MER maximization is due to restriction by its lower value range and due to maximal air flow rate constraint in upper refrigerant flow rate. The maximal air flow rate constraint applies for all points starting from maximal SMER value through the upper range of refrigerant flow rate for SMER maximized cycle.

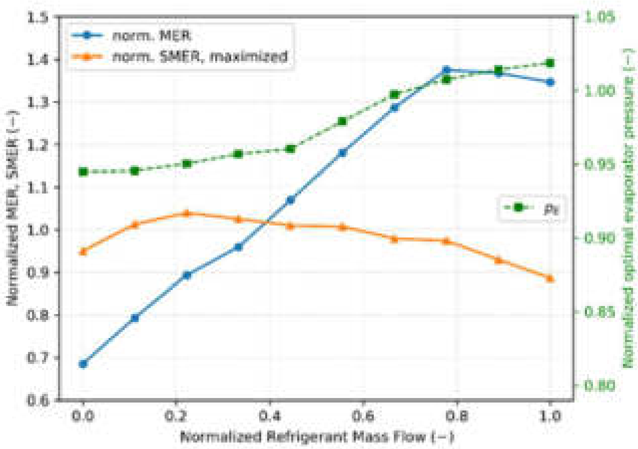

Figure 9 Optimal performance of vented cycle for SMER objective function

5 Conclusions

A thermodynamic model of closed and vented heat pump drying cycle have been described. Optimization results for drying performance parameters; drying rate - MER and energy efficiency - SMER parameters for both cycles have been analysed in the paper.

Results of the optimization showed strong correlation of the MER parameter with refrigerant flow rate for both closed and vented heat pump drying cycle. There is same maximal MER value obtained for both MER and SMER optimized cycle parameters. The difference in optimal SMER value accounts only for 2% difference between SMER and MER optimized cycles.

It has been shown that refrigerant and air flow rate are dependent parameters for vented heat pump drying cycle. Optimized parameters of vented cycle showed better drying performance compared to closed cycle. There is computed improvement of more than 10% and 4% for MER and SMER parameters, respectively.

Acknowledgement

This article was supported by the projects KEGA 033ŽU-4/2018 "Heat sources and pollution of the environment", APVV-17-0311 "Research and development of zero waste technology for the decomposition and selection of undesirable components from process gas generated by the gasifier" and VEGA 1/0233/19 "Construction modification of the burner for combustion of solid fuels in small heat sources".

References

[1] MINEA, V.: *Advances in Heat pump-assisted dring tehcnology*, CRC Press, 2016.

[2] CONDE M.: Energy conservation with tumbler drying in laundries, *Applied Thermal Engineering*; Vol. 17, No. 12, pp. 1163-72, 1997.

[3] LAMBERT, A. J. D., SPRUIT, F. P. M., CLAUS, J.: Modelling as a Tool for Evaluating the Effects of Energy-Saving Measures. Case Study: A Tumbler Drier, *Applied Energy,* Vol. 38, No. 1, pp. 33-47, 1991.

[4] HEKMAT, D., FISK, W.J.: *Improving the energy performance of residential clothes dryers*, 35th Annual international applience technical conference Ohio state univrsity, 1984.

[5] BANSAL, P. K., BRAUN, J. E., GROLL, E. A.: Improving the energy efficiency of conventional tumbler clothes drying systems, *International Journal of Energy Research*, Vol. 25, No. 15, pp 1315-1332, 2001.

[6] TAUŠ, P., TAUŠOVÁ, M., ŠLOSÁR, D., JEŇO, M., KOŠČO, J.: Optimization of energy consumption and cost effectiveness of modular buildings by using renewable energy sources, *Acta Montanistica Slovaca*, Vol. 20, No. 3, pp. 200-208, 2015.

[7] SAENSABAI, P., PRASERTSAN, S.: Effects of Component Arrangement and Ambient and Drying Conditions on the Performance of Heat Pump Dryers, *Drying Technology: An International Journal*, Vol. 21, No. 1, pp. 103-127, 2003

[8] CARRINGTON, C.G., BANNISTER, P., LIU, Q.: Performance of a scroll compressor with R134a at medium temperature heat pump conditions, *International journal of energy research*, Vol. 20, No. 8, pp. 733-743, 1996.
[9] KOŠČO, J., KUDELAS, D., TAUŠ, P.: *Aplication of 1 MW heat pump york 0955HA and analysys of problems in audit of procedure*, SGEM 2016, Albena, STEF92 Technology Ltd., pp. 139-145, 2016.

Review process

Single-blind peer review process.

Acta Tecnología - International Scientific Journal about Technologies
Volume: 5 2019 Issue: 4 Pages: 93-96 ISSN 2453-675X

doi:10.22306/atec.v5i4.64

Received: 10 Oct. 2019
Accepted: 12 Nov. 2019

EVALUATION METHODS OF BONE CONDITION

Kornelia Zaborowska
University of Zielona Góra, Department of Physics, ul. Szafrana 2, P.O.Box 47, 65-516 Zielona Góra, Poland, EU, kornelia.zaborowska@gmail.com
Marianna Trebuňová
Technical University of Košice, Faculty of Mechanical Engineering, Department of Biomedical Engineering and Measurement, Letná 9, 042 00 Košice, Slovak Republic, EU, marianna.trebunova@tuke.sk (corresponding author)
Piotr Kuryło
University of Zielona Góra, Department of Mechanics, ul. Szafrana 2, P.O.Box 47, 65-516 Zielona Góra, Poland, EU, P.Kurylo@ibem.uz.zgora.pl
Piotr Pruszyński
105th Borderlands Military Hospital of Żary, Orthopaedic & Trauma Surgery Department, ul. Domańskiego 2 68-200 Żary Poland, EU, ppruszi@wp.pl
Joanna Cyganiuk
University of Zielona Góra, Department of Mechanics, ul. Szafrana 2, P.O.Box 47, 65-516 Zielona Góra, Poland, EU, J.Cyganiuk@ibem.uz.zgora.pl
Peter Frankovský
Technical University of Košice, Faculty of Mechanical Engineering, Department of Applied Mechanics and Mechanical Engineering, Letná 9, 042 00 Košice, Slovak Republic, EU, peter.frankovský@tuke.sk

Keywords: osteoporosis, dual energy X-ray absorptiometry, quantitative ultrasound, single energy X-ray absorptiometry, quantitative computed tomography

Abstract: The article presents research methods for bone damage diagnosis by osteoporosis. We describe in detail densitometric methods such as DEXA tests, SXA method, Quantitative Computed Tomography (QCT) and Quantitative UltraSound (QUS) method. In this article we evaluated to problems concerning in diagnosis and the availability of diagnostic equipments.

1 Introduction

The person has bones in the best physiological state between 20-40 years old. When a bone fracture occurs, the process of its reconstruction occurs. This means that the bone itself can replace damaged structures. Low-energy fractures are most common in people with increasing age. It is mainly about the fractures of the spine, the neck of the femur and the wrist. A low-energy break is a fracture caused by the relatively small forces that would not occur under normal conditions, ie without tissue weakening. The cause of the fracture is the lack of bone remodelling itself. One of the causes is calcium depletion. It is a condition where bone absorbs calcium more quickly and its replenishment is relatively slow. The bones lose their density. Osteoporosis is most diagnosed in the case of a first fracture. Osteoporosis develops asymptomatically, relieving the skeleton of stored calcium sources. Patients who have already had their first fractures and at-risk patients will be selected for a series of tests to diagnose osteoporosis. Therefore, these tests can be divided into four main categories (Figure 1).

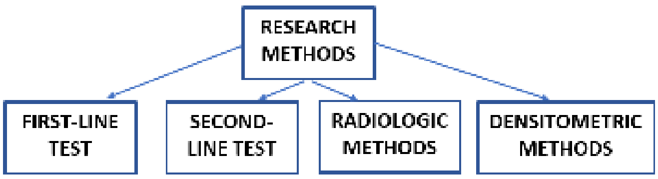

Figure 1: Bone research methods for the diagnosis of osteoporosis

The **first-line tests** include the determination of ESR (*erythrocyte sedimentation rate*) levels, alkaline phosphatase activity and the levels calcium and phosphorus in serum. The erythrocyte sedimentation rate (ESR) is a measure of the rate at which red blood cells fall and is an indicator of a possible inflammation. Basic alkaline phosphatase is an enzyme found in bones, liver and intestines [1].

The **second-line tests** may include tests for monoclonal protein in blood to exclude multiple myeloma, PTH concentration (Parathormone is a parathyroid hormone responsible for calcium-phosphate metabolism), 1,25$(OH)_2$D, and osteocalcin which demonstrates the quality of bone turnover. And the determination of levels of calcium and hydroxyproline excreted from urine [2].

2 Methodology

Radiologic methods are based on the use of X-rays. Osteoporosis is most often diagnosed by detecting typical fractures or deformities, especially within the vertebrae. Lesions occurring before a fracture has occurred are visible only in the case of the loss in bone mass of the order of 30 ÷ 50%. The most common fractures occur in the lower and upper bone shafts. Further development of osteoporosis results in wedge shaped fractures occurring in the front parts, most often in the thorax. In the last stage of the disease, frequent occurrence of vertebrae crushes, i.e. compression fractures were observed. X-ray based methods do not allow for a direct quantitative analysis of bone calcification, and any evaluation attempts depend significantly on the subjective opinion of a radiologist evaluating the image. Individual parameters of X-ray emitting lamps also affect the evaluation possibilities. However, tests of this group may be enough to diagnose osteopenia, i.e. local diminished bone density, which is the basis for ordering further densitometry tests [3-5].

Densitometric tests are designed to determine the quantitative bone loss. The tests in this group consist of measuring the amount of absorbed X-ray that passes through the examined bones by comparing the amount of radiated energy and the amount that reaches the detector. Densitometric tests can be divided by the location of the measurements: SXA, QCT, QUS and DEXA (Figure 2). Densitometric tests use significantly lower radiation doses than standard x-ray examinations [6-9].

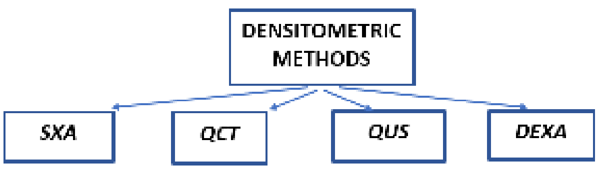

Figure 2: Densitometric tests by the location of measurements, where SXA – (Single Energy X-ray Absorptiometer); QCT – (Quantitative Computed Tomography); QUS – (Quantitative UltraSound); DEXA – (Dual Energy X-ray Absorptiometry)

The ***DEXA*** tests (Dual Energy X-ray Absorptiometry) - allow the evaluation of density parameters of central parts of the skeleton. Tests in this group are called bi-energetic X-ray densitometry. They are used to analyse the density of the lumbar spine, the femur, and to determine the average density of the entire skeleton. In this test method, the BMD (*Bone Mineral Density)* parameter, expressed in [g/m^3], is determined. The result may be presented in three forms and is a reference for former tests for a given population. Two of the forms are expressed as percentage values. The first one is the reference for the bones of the young (% young adult), whereas the second - is the reference for the peak bone density (% age matched), or in a form of a number of standard deviations (Z-score), which refers to gender and age [10,11].

The most studied human motoric organ is the spine in the lumbar region and the femur (right or left). Diagnosed areas in the spine are most often selected due to their presence in both trabecular and solid structures. Areas of the femur are examined due to the most commonly occurring fractures. In these areas, osteoporosis can be diagnosed by defining a standard deviation below T-Score -2,5 [12].

With the DEXA X-ray densitometry method, the radiation beam consists of isolated groups of low and high energy photons that allow bone analysis neglecting the soft tissue composition. A narrow-angle fan beam is used which, after passing through the tissue, falls on the scintillator which allows further segmentation of the image. The basic element of the densitometer is X-ray micro tube and a sensor measuring the intensity of radiation [13].

Contrary to the single energy X-ray absorptiometer (***SXA***) method, in this method the tested areas do not need to be immersed in water to eliminate the effect of soft tissue. The DEXA (Dual Energy X-ray Absorptiometry) uses alternating low and high energy radiation. The absorption of these types of radiation is significantly different for soft tissues and almost identical for bones. The separation between the spongy and compact osseous tissues is not taken into consideration in the analysis. Based on these differences between bones and the surrounding tissues, the influence of soft tissue is eliminated. The DEXA densitometers are also available in peripheral versions for examining the bones of the forearm, phalanges and heels. They practically replaced the SXA apparatuses in the market. The main disadvantage of peripheral densitometry is the lack of ability to perform examinations of the vertebral and the proximal part of the femur, i.e. areas where earliest bone losses occur and where life-threatening fractures are most common [14].

Quantitative Computed Tomography (***QCT***) uses much higher doses of ionizing radiation than DEXA densitometers. The radiation source revolves around the patient's body, and the output radiation is recorded by the detector matrix. The test is more burdensome for the patient but allows the determination of the actual bone density expressed in mg/m^3. However, its cost significantly outweighs other diagnostic methods. The density value is analysed directly for each voxel. It is possible to evaluate separately the properties of the cortical bone, and separately – of the compacted bone. Appliances for this type of tests are dedicated appliances, or ordinary computer tomographs with additional software [15].

The Quantitative UltraSound (***QUS***) method is used for testing of the patella, the phalanges or the heel, i.e. in areas where there is little surrounding soft tissue [16].

The examination includes two parameters, i.e. the speed of sound (SOS) and the Broadband Ultrasound Attenuation (BUA). SOS is the velocity of the ultrasonic wave that changes while penetrating bone structures thus reflecting the density of the bone. BUA is the weakening of the ultrasonic wave dependant mainly on the bone structure, i.e. the trabecular thickness, the number of inter-trabecular spaces and the direction of the arrangement. The test results based on ultrasound are significantly different from those obtained using RTG radiation, but the method is much cheaper and simpler. Ultrasonography is mainly used in screening. An ultrasound transducer emits ultrasounds (with the use of piezoelectric elements). On the other side of the tested object, there is a sensor that measures the values of the beam after its passage through the bone. Acoustic properties of the bone are determined. The more porous and heterogeneous it is, the greater is the weakening and the slowing of the beam [17,18].

3 Problems in diagnosis and availability of diagnostic equipment

It is the primary care physicians who can most effectively reach the population at risk of damage bone, identify the disease and treat it. In many health care's centres, doctors do not have enough time to thoroughly examine a patient. Medical interviews are not carried out precisely enough because of long queues of patients. Doctors are reluctant to direct patients for additional, adjunctive testing that can accurately diagnose osteoporosis. The main reason lies in financial resources, but also in doctors' inadequate knowledge. Medical centres, in order to save on specialized tests, usually send patients to x-rays (*RTG – Radioisotope Thermoelectric Generator or roentgenogram).* As a rule, medical centres are equipped with such devices, which minimize the cost of sending patients to more specialized tests, especially if they are to be performed by their competitors. A patient who goes to see their GP is sent to an RTG in the first place. A radiology technician performs an x-ray, and a radiology doctor describes the changes visible in the image. It is assumed that osteoporosis-specific radiological changes are only visible when 30% to 50% of bone mass has been lost. It should be noted that X-ray is not the appropriate method for determining the degree of bone loss without fractures. The test does not allow for the quantitative analysis of the skeleton calcification. Radiologists with longer work experience determine minor bone decay as osteopenia and advanced stages of bone changes as osteoporosis. Thinner bodies mean the reduction of the thickness of their spinal cord border as well as vertical bands characterizing disappearance of the horizontal trabeculae in the bone structure may suggest low bone mass. The assessment of such changes is often subjective and largely depends on the setting of the X-ray tube parameters [19].

The availability of specialized examinations for the patient is also problematic. In most cases, osteoporosis is diagnosed only after a pathologic fracture, so at the stage where there is significant bone mass loss and bone weakening. The prevention and screening system for the possible largest number of patients, especially those with the highest risk, should be implemented. National healthcare institutions should develop a system based on cheaper test methods, safer, more repeatable and more precise, i.e. methods which would combine the advantages of ultrasonographic tests and x-ray [20,21].

4 Summary and conclusion

There are a considerable number of diseases weakening the mechanical properties of bones in humans.

The most common of them is osteoporosis, which, if diagnosed early, allows for a long life without motoric disability or other complications. Therefore, it is important to diagnose it early, at a stage in which it does not cause pathological fractures. Among a large number of possible screening tests, methods which are inert for the human body are the ultrasound examinations. However, as these tests show little accuracy, they should be supplemented, if there are any doubts, with the DEXA method, which uses low radiation energies. These methods have a negligible impact on the human body, and the benefits of their accuracy far outweigh the risks associated with X-rays [22,23].

Acknowledgment

This article was supported by the state grant KEGA 69TUKE-4/2017, VEGA 1/0316/18 of the Ministry of Education of the Slovak Republic and APVV-17-1258.

References

[1] MAILLEFERT, J. F., AHO, L. S., EL MAGHRAOUI, A., DOUGADOS, M., ROUX, C.: Changes in bone density in patients with ankylosing spondylitis: a two-year follow-up study, *Osteoporosis International*, Vol. 12, No. 7, pp. 605-609, 2001.

[2] RASMUSSEN, H., BORDIER, P., MARIE, P., AUQUIER, L., EISINGER, J. B., KUNTZ, D., CAULIN, F., ARGEMI, B., J. GUERIS, A. J.: Effect of combined therapy with phosphate and calcitonin on bone volume in osteoporosis, *Metabolic Bone Disease and Related Research*, Vol. 2, No. 2, pp. 107-111, 1980.

[3] ZUKIĆ, D., VLASÁK, A., EGGER, J., HOŘÍNEK, D., NIMSKY, C., KOLB, A.: Robust detection and segmentation for diagnosis of vertebral diseases using routine MR images, *Computer Graphics Forum,* Vol. 33, No. 6, pp. 190-204, 2014.

[4] DAMILAKIS, J., ADAMS, J. E., GUGLIELMI, G., LINK, T. M.: Radiation exposure in X-ray-based imaging techniques used in osteoporosis, *European radiology*, Vol. 20, No. 11, pp. 2707-2714, 2010.

[5] LIMA, I., ANJOS, M. J., FLEIUSS, M. L. F., ROSENTHAL, D., LOPES, R. T.: Characterization of osteoporotic bone structures by bidimensional images through x-ray microfluorescence with synchrotron radiation, *X-Ray Spectrometry: An International Journal*, Vol. 37, No. 3, pp. 249-254, 2008.

[6] BOUSSON, V., LE BRAS, A., ROQUEPLAN, F., KANG, Y., MITTON, D., KOLTA, S., BERGOT, C., SKALLI, W., VICAUT, E., KALENDER, W., ENGELKE, K., LAREDO, J.D.: Volumetric quantitative computed tomography of the proximal femur: relationships linking geometric and densitometric variables to bone strength. Role for compact bone, *Osteoporosis International*, Vol. 17, No. 6, pp. 855-864, 2006.

[7] ZLATARIĆ, D. K., ČELEBIĆ, A.: Clinical bone densitometric evaluation of the mandible in removable denture wearers dependent on the morphology of the mandibular cortex, *The Journal of prosthetic dentistry*, Vol. 90, No. 1, pp. 86-91, 2003.

[8] KANIS, J. A., GLÜER, C. C.: An update on the diagnosis and assessment of osteoporosis with densitometry, *Osteoporosis International*, Vol. 11, No. 3, pp. 192-202, 2000.

[9] BONNICK, S. L., LEWIS, L. A.: *Bone densitometry for technologists,* Totowa, NJ: Humana Press., pp. 67-94, 2006.

[10] BLAKE, G. M., FOGELMAN, I.: Role of dual-energy X-ray absorptiometry in the diagnosis and treatment of osteoporosis, *Journal of Clinical Densitometry*, Vol. 10, No. 1, pp.102-110, 2007.

[11] BECK, T.: Measuring the structural strength of bones with dual-energy X-ray absorptiometry: principles, technical limitations, and future possibilities, *Osteoporosis International*, Vol. 14, No. 5, pp. 81-88, 2003.

[12] KRUEGER, D., FIDLER, E., LIBBER, J., AUBRY-ROZIER, B., HANS, D., BINKLEY, N.: Spine Trabecular Bone Score (TBS) Subsequent to BMD Improves Fracture Discrimination in Women, *Journal of Clinical Densitometry*, Vol. 15, No. 4, pp. 482, 2012.

[13] KHALID, A. A., MARGHANI, A., HUSSEIN, B., MOHAMMED, H. A., MAJDI, M.: Measurement of Normal Bone Density for Sudanese Patients Using Computed Tomography, 2015.

[14] RAMOS, R. L., ARMÁN, J. A., GALEANO, N. A., HERNÁNDEZ, A. M., GÓMEZ, J. G., MOLINERO, J. G.: Dual energy X-ray absorptiometry: fundamentals, methodology, and clinical applications, *Radiología (English Edition)*, Vol. 54, No. 5, pp. 410-423, 2012.

[15] ADAMS, J. E.: Quantitative computed tomography, *European journal of radiology*, Vol. 71, No. 3, pp. 415-424, 2009.

[16] LAUGIER, P.: Instrumentation for in vivo ultrasonic characterization of bone strength. *IEEE transactions on ultrasonics, ferroelectrics, and frequency control*, Vol. 55, No. 6, pp. 1179-1196, 2008.

[17] GLUER, C. C., WU, C. Y., JERGAS, M., GOLDSTEIN, S. A., GENANT, H. K.: Three quantitative ultrasound parameters reflect bone structure. *Calcified tissue international*, Vol. 55, No. 1, pp. 46-52, 1994.

[18] GRAAFMANS, W. C., LINGEN, A. V., OOMS, M. E., BEZEMER, P. D., LIPS, P.: Ultrasound measurements in the calcaneus: precision and its relation with bone mineral density of the heel, hip, and lumbar spine, *Bone*, Vol. 19, No. 2, pp. 97-100, 1996.

[19] CNUDDE, V., BOONE, M. N.: High-resolution X-ray computed tomography in geosciences: A review of the current technology and applications, *Earth-Science Reviews*, Vol. 123, No. August, pp. 1-17, 2013.

[20] HOHLWEG-MAJERT, B., SCHMELZEISEN, R., PFEIFFER, B. M., SCHNEIDER, E.: Significance of osteoporosis in craniomaxillofacial surgery: A review of the literature, *Osteoporosis international*, Vol. 17, No. 2, pp. 167-179, 2006.

[21] GUELDNER, S. H., GRABO, T. N., NEWMAN, E. D., COOPER, D. R. (Eds.).: *Osteoporosis: clinical guidelines for prevention, diagnosis, and management,* Springer Publishing Company, 2007.

[22] HEINI, P. F.: The current treatment—a survey of osteoporotic fracture treatment. Osteoporotic spine fractures: the spine surgeon's perspective, *Osteoporosis international*, Vol. 16, No. 2, pp. 85-92, 2005.

[23] HOHLWEG-MAJERT, B., SCHMELZEISEN, R., PFEIFFER, B. M., SCHNEIDER, E.: Significance of osteoporosis in craniomaxillofacial surgery: A review of the literature, *Osteoporosis international*, Vol. 17, No. 2, pp. 167-179, 2006.

Review process

Single-blind peer review process.

Acta Tecnología - International Scientific Journal about Technologies
Volume: 5 2019 Issue: 4 Pages: 97-102 ISSN 2453-675X

doi:10.22306/atec.v5i4.66

Received: 05 Dec. 2019
Accepted: 28 Dec. 2019

MOTION ANALYSIS OF POINT OF A SIMPLE MECHANISM

Darina Hroncová
Technical University of Kosice, Faculty of Mechanical Engineering, Letna 9, Kosice, Slovak Republic, EU, darina.hroncova@tuke.sk (corresponding author)
Ingrid Delyová
Technical University of Kosice, Faculty of Mechanical Engineering, Letna 9, Kosice, Slovak Republic, EU, ingrid.delyova@tuke.sk

Keywords: kinematics, analytical solution, numerical solution, simulation
Abstract: This article deals with motion analysis of point of a simple mechanism executing a rotational movement. We analysed the movement of its end points. The trajectories of points is cardioids. Numerical solution was implemented by classical kinematics using different coordinate systems, while model mechanism has been also modelled and solved in the program MSC ADAMS View.

1 Introduction

In addressing the motion of machine parts, machines and equipment it is necessary to first create a kinematic model. Kinematic model of a device schematically captures all its properties which are essential in kinematic analysis i.e. individual members with dimensions, kinematic pairs, and so on [1-5].

Conventional numerical solution uses vector calculus as the basic mathematical apparatus because the main kinematic variables are vector quantities.

For analytical kinematic analysis of movement different coordinate systems may be used. According to the kind of movement we can choose the appropriate coordinate system for that model configuration thus simplifying the solution [3-8].

Classical numerical solution of movement kinematics is often lengthy and difficult especially for complex kinematic models with different movements. To simplify and expedite solutions a graphical solution may be used which is nowadays replaced with a solution using computer techniques using various software products. These software products ease the investigator's effort. Investigator enters the model configuration and the input data and the program calculates the required outputs. These data can be presented in a tabular form or program draws graphical results. One of the software products suitable for kinematic analysis is MSC ADAMS View program that allows to model kinematic chains and solve their motion [9-13].

2 Cardioid motion

Conchoidal movement is if the line p of the moving body passes through the point of the base frame C (the central point - the pole of movement) and the body point Q describes the control curve q (Figure 1).

The trajectories of body points are called conchoids. Conchoidal motion is a special case of point-to-curve motion. If the central point lies on the control circle, this is a special case where point C is still the vertex of the right angle of the triangle above the diameter QP. The stationary polodia k_1 is a circle identical to the driving circle ($q = k_1$). The driving polodia is the circle with the double radius k_2. It is a cardioid movement.

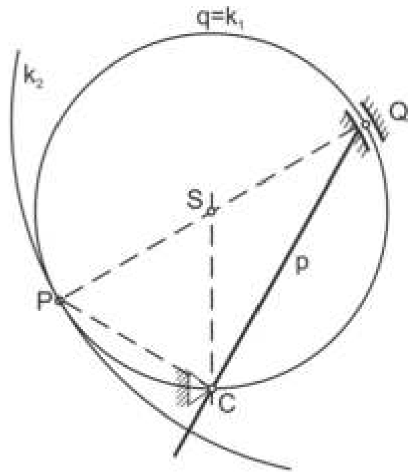

Figure 1 Point-to-curve motion

Cardiodic motion is said if each of the selected body lines passes a given point of the base frame. Each line connected to the body and passing through the point Q will slide over the point of the base frame C lying on the stationary polodia. Every movement of the body whose two lines slide along the base frame circle is cardioid.

Inversion of elliptical motion is obtained by:

a) moving the sides of an angle of constant size through two fixed points,
b) rolling a circle on another of half the size fixed inside it,
c) as a result of (a) and (b), making a point Q on a line CQ trace a circle, whilst so constraining this line that it continues to pass through a fixed point C on the circle.

The pole is invariably diametrically opposite the moving point O on the fixed circle.

Such motion is called cardioid because the paths of points involved are heart-shaped or of a shape derived from this (Figure 2). The diagram shows a line C_1AC_2 having a point A which traces the fixed circle k_1, whilst the line itself invariably passes through the fixed point B on circle k_1 [14].

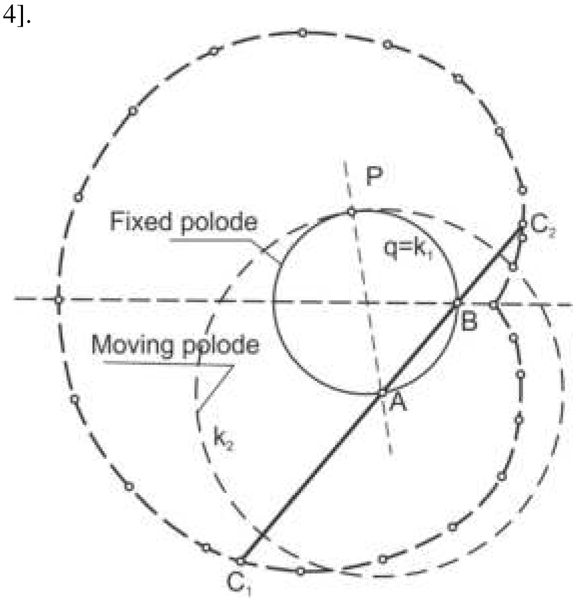

Figure 2 Cardioid motion

3 Point movement example

We analyse the movement of point C on the line p, Figure 3. The line p is moving in the plane $0, x, y$ so that it always goes through the point 0, the point A of the line p moves in a circle with a radius R. The angular velocity of the line p is $\omega = const. > 0$. In time $t_0 = 0$ is $p \equiv x, \overline{AC} = 2R$.

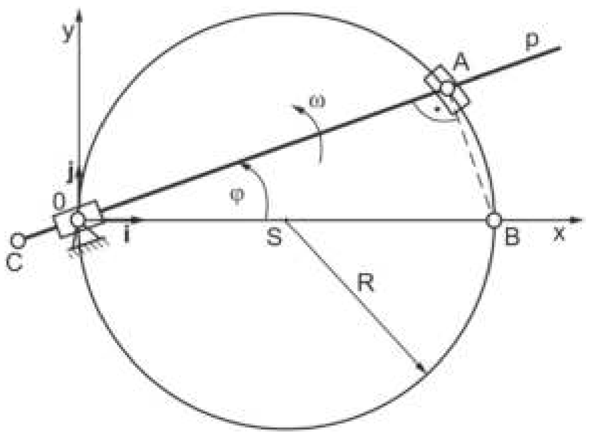

Figure 3 Mechanical system

Line p carries out a uniform rotational motion around the point 0 and in time $t_0 = 0$ is $p \equiv x$.

By introduction of the polar coordinate system we get $\rho = \rho(t), \varphi = \varphi(t)$.

Since $\omega = const.$, then $\varphi = \omega t$.

From triangle 0AB we get (1) $\rho = \overline{0A}$, and

$$\rho = 2R\cos\varphi = 2R\cos\omega t\,. \qquad (1)$$

Polar coordinates ρ, φ of the point A of line p in time t are given by following (2):

$$\varphi = \omega t, \;\; \rho = 2R\cos\omega t \qquad (2)$$

Position vector (3) r of the point A of line p in time t using Cartesian coordinate system is given by:

$$\mathrm{r} = x\mathrm{i} + y\mathrm{j}, \qquad (3)$$

where x,y (4), (5) are coordinates of the point A of line p in time t are according to the picture:

$$x = \rho\cos\varphi = 2R\cos^2\omega t \qquad (4)$$
$$y = \rho\sin\varphi = 2R\cos\omega t\sin\omega t \qquad (5)$$

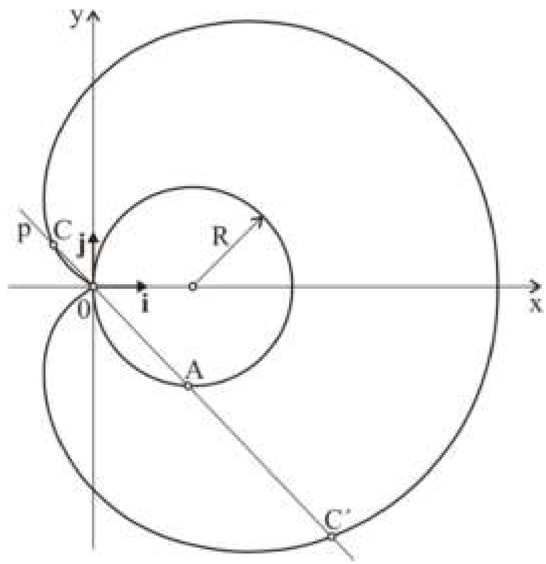

Figure 4 Trajectories of points A and C

Position vector (6) is

$$r = (2R\,cos^2\,\omega t)i + (2R\,cos\,\omega t\,sin\,\omega t)j. \qquad (6)$$

To be able to determine the trajectory of point C, we need to know the parametric equations of the trajectory given by the coordinates of C in relation to time t [15,16]

The coordinates of the point C can be determined (7), (8) from the image

$$x_C = -\overline{0C}\cos\varphi = -\overline{0C}\cos\omega t, \qquad (7)$$
$$y_C = -\overline{0C}\sin\varphi = -\overline{0C}\sin\omega t. \qquad (8)$$

The distance $\overline{0C} = \overline{AC} - \overline{0A}$, while (9), (10)

$$\overline{AC} = 2R, \qquad (9)$$
$$\overline{0A} = \rho = 2R\cos\omega t. \qquad (10)$$

By modification we get the coordinates (11), (12) or parametric equations of the trajectory of the point C.

$$x_C = -2R(1 - \cos\omega t)\cos\omega t, \quad (11)$$
$$y_C = -2R(1 - \cos\omega t)\sin\omega t. \quad (12)$$

Eliminating the parameter t from the parametric equations we get the equation (13) of trajectory of point C

$$(x^2 + y^2 - 2Rx)^2 = 4R^2(x^2 + y^2). \quad (13)$$

Resulting equation is the equation of a cardioid. The trajectory of the point C is thus a cardioid, Figure 4.

4 Simulation in MSC ADAMS View

MSC ADAMS View allows to model, analyse and optimize virtual prototypes of future products, investigate their properties before producing the real prototype and now covers over 50% of the world market in its area. It is also an appropriate tool for the development of miniature mechatronic elements as well as the examination of complex systems.

The given mechanism was modelled in MSC ADAMS View and the initial parameters were provided. In Figure 5 there is the model in motion with trajectories of points A and C.

In Figure 6 there is the position vector of the point C in time t and in Figure 7 is the position vector of the point A in time t, velocity and acceleration. Trajectory of the point C is in Figure 8 and Figure 9.

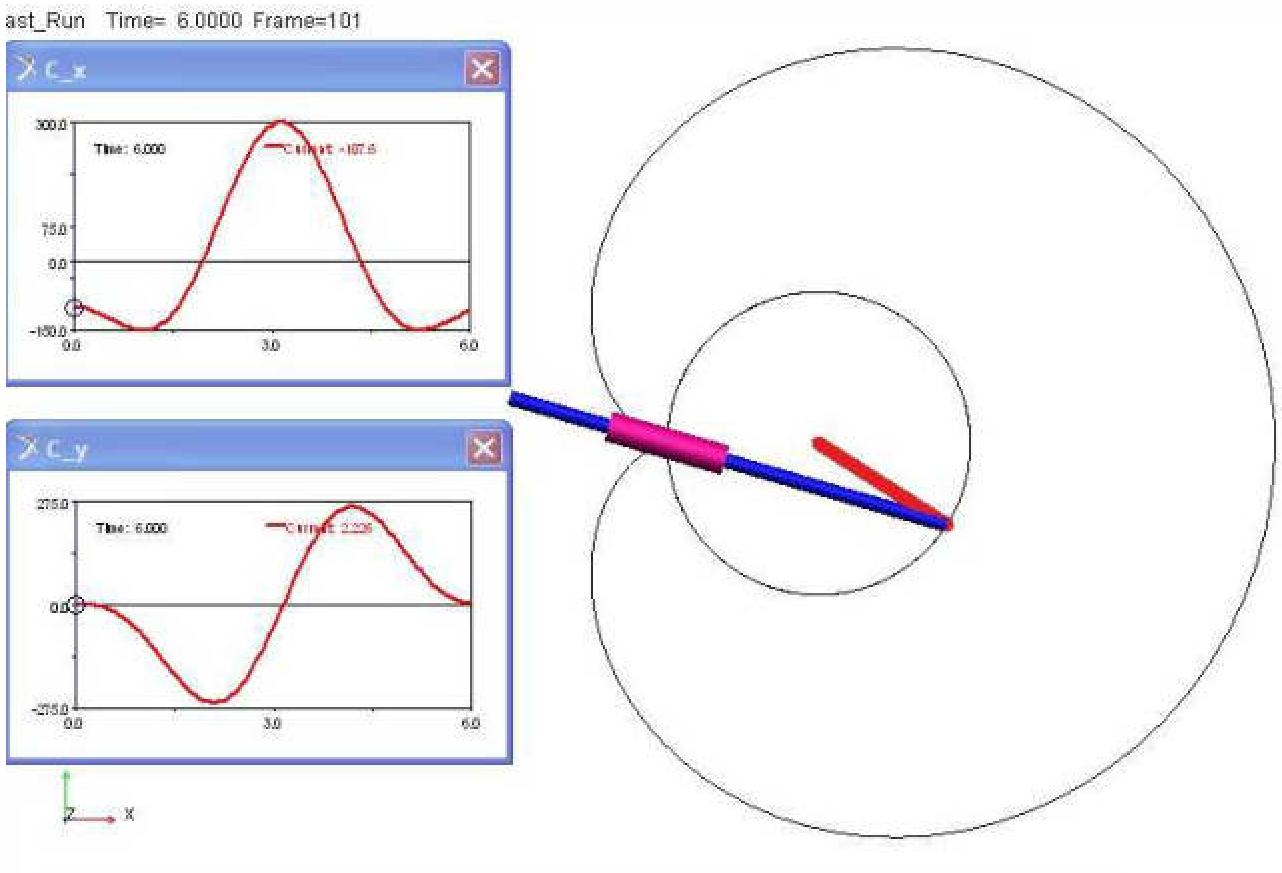

Figure 5 Position of the mechanism in the movement

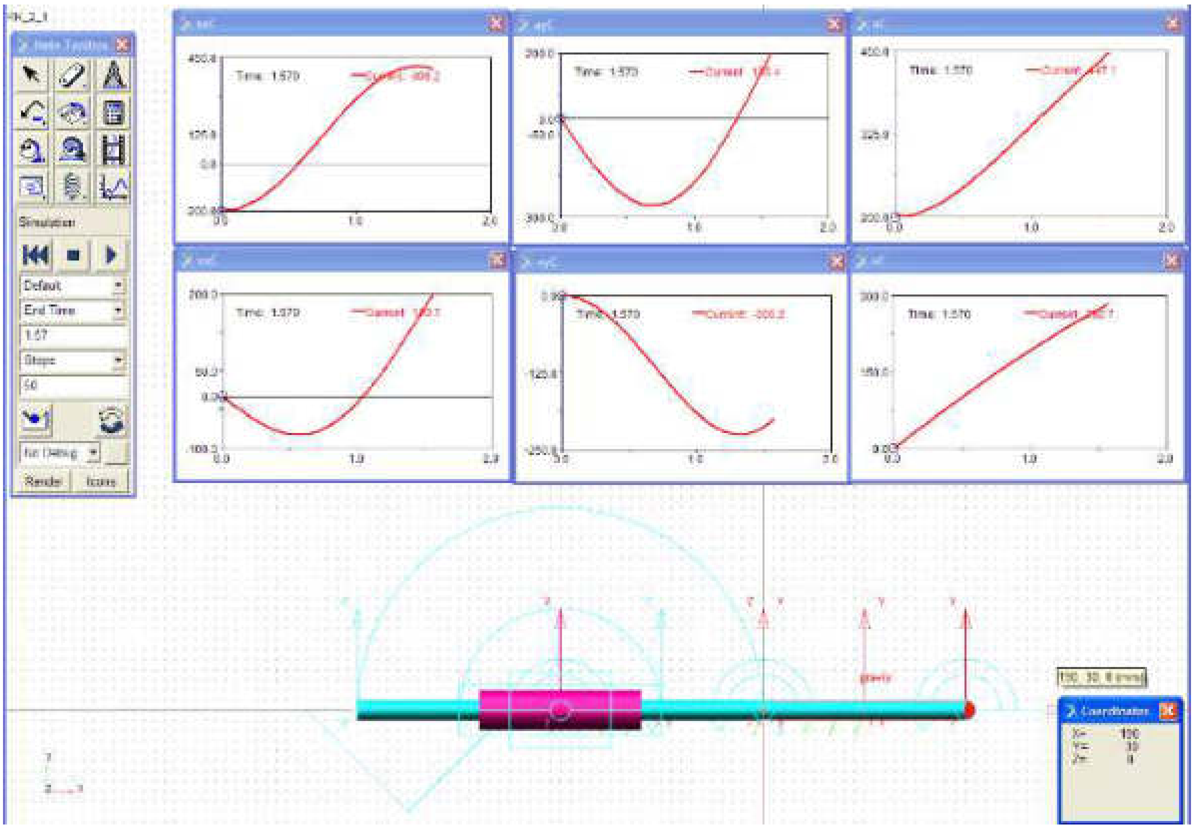

Figure 6 Speed and acceleration of the points C

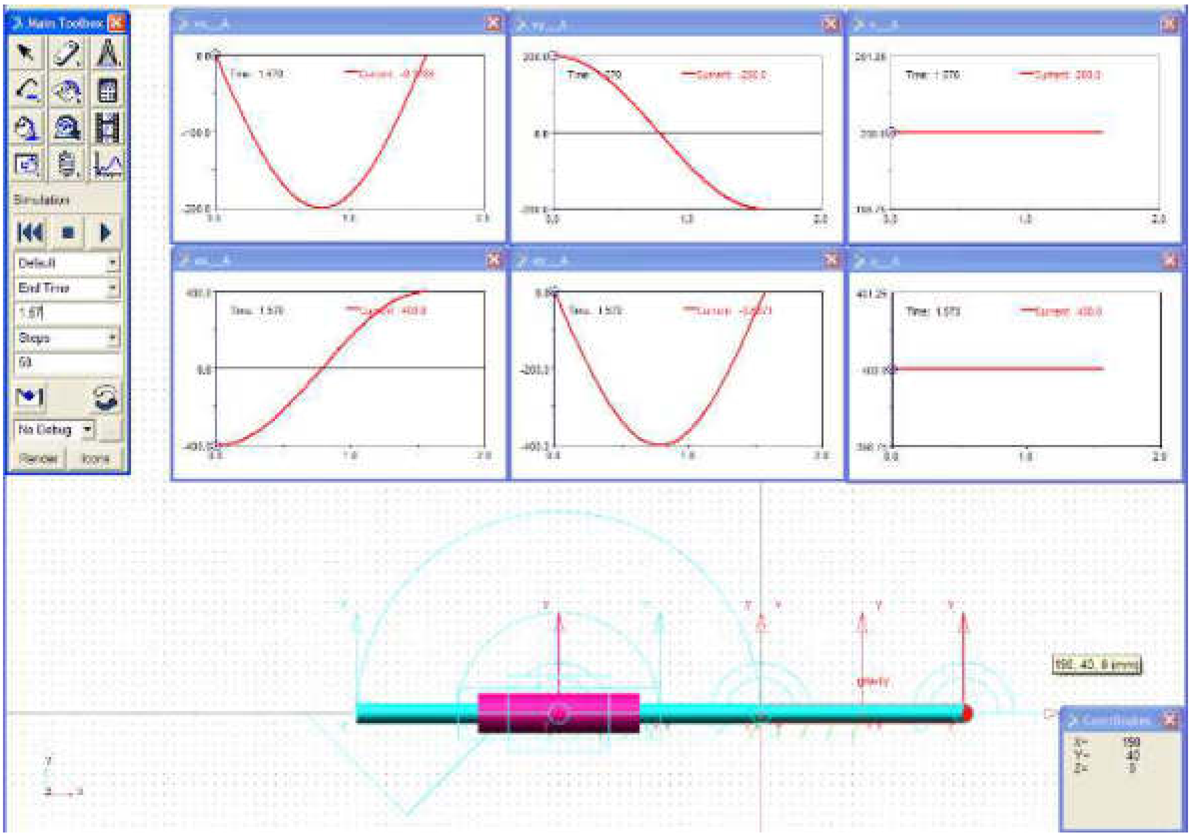

Figure 7 Speed and acceleration of the points A

Volume: 5 2019 Issue: 4 Pages: 97-102 ISSN 2453-675X

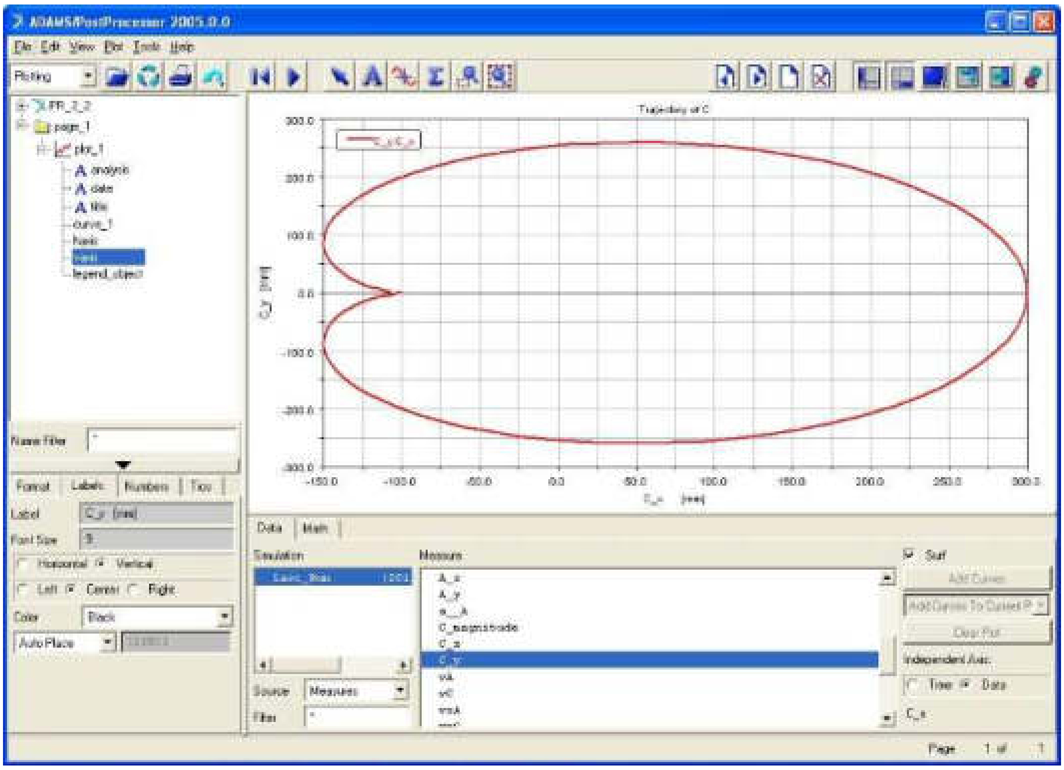

Figure 8 ADAMS PostProcessor

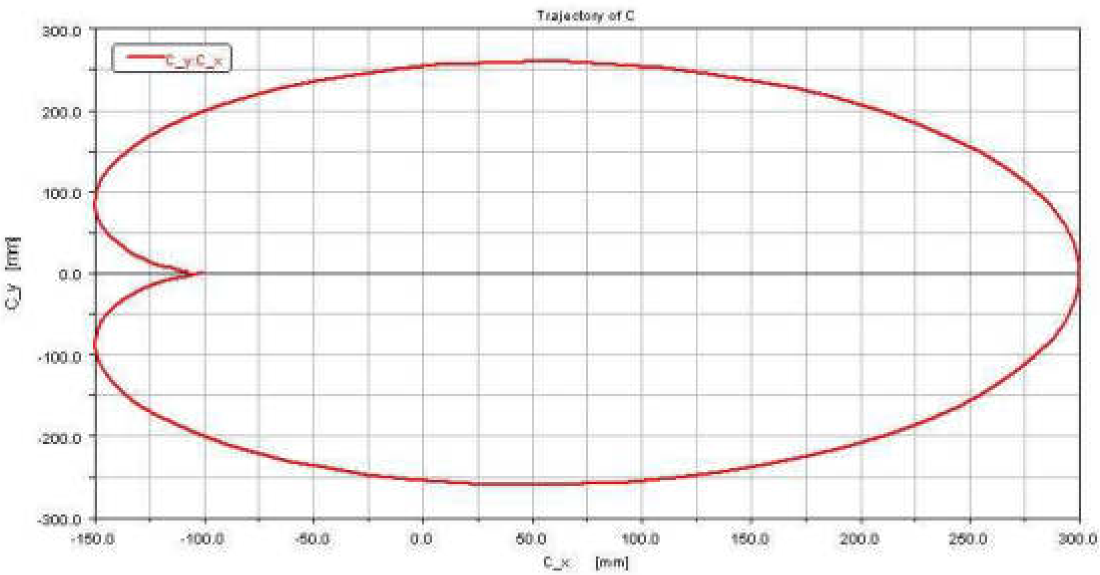

Figure 9 Trajectory of the point C in x-y plane

5 Conclusion

In the work is shown a procedure for solving kinematic problem of the mechanism using analytical solution and modelling in MSC Adams View. MSC Adams View allows to simulate moving of such mechanical systems. Results are obtained in form of time diagram of the desired variables. Tasks are solved numerically, model is compiled by using program MSC Adams View. Mastering this methodology provides a suitable tool for solving problems of teaching and practice.

Acknowledgement
The authors would like to thank to Slovak Grant Agency – project VEGA No. 1/0290/18, VEGA No. 1/0872/16 VEGA No. 1/0389/18, KEGA No. 049TUKE-4/2017 and grant project KEGA No. 018TUKE-4/2018 supported by the Ministry of education of Slovak Republic.

References

[1] JULIŠ, K., BREPTA, R.: *Mechanics II*, Dynamics, Praha, SNTL, 1987. (Original in Czech)

[2] SHABANA, A.A.: *Dynamics of Multibody Systems,* 2nd ed., Cambridge University Press, 1998.

[3] SHABANA, A.A.: *Computational Dynamics,* 2nd ed., John Wiley & Sons, Inc., New York 2001.

[4] CHYNORADSKÝ, L., BOŽEK, P.: Research and development of a new system of the autonomous control of robot trajectory, *Acta Mechatronica*, Vol. 1, No. 1, pp. 25-28, 2016.

[5] STEJSKAL, V., VALÁŠEK, M.: *Kinematics and dynamics of Machinery*, Marcel Dekker, Inc., New York, 1996.

[6] WALDRON, K.J., KINZEL, G.L.: *Kinematics, Dynamics and Design of Machinery*, John Wiley & Sons, Inc., New York, 1999.

[7] HRONCOVÁ, D., BINDA, M., ŠARGA, P., KIČÁK, F.: Kinematical analysis of crank slider mechanism using MSC Adams/View, *Procedia Engineering*, Vol. 48, pp. 213-222, 2012.

[8] HRONCOVÁ, D., FRANKOVSKÝ, P., VIRGALA, I., DELYOVÁ, I.: Kinematic Analysis of the Press Mechanism Using MSC Adams, *American Journal of Mechanical Engineering*, Vol. 2, No. 7, pp. 312-315, 2014.

[9] XIONG, W., CHEN, Z. T., WU, H., XU, G., DING, T., MEI, H. P., LI, Y. M.: Solution to the motion of a delta manipulator with three degrees of freedom, *Ferroelectrics*, Vol. 529, No. 1, pp. 159-167, 2018.

[10] ENESCU, M.: Finite Element Analysis of an industrial robot within the MSC.ADAMS software, *Bulletin of the Transilvania University of Braşov*, Vol. 9, No. 2, pp. 119-124, 2016.

[11] DELYOVÁ, I., HRONCOVÁ, D., FRANKOVSKÝ, P., DZURIŠOVÁ, E., RÁKAY, F.: Kinematic analysis of crank rocker mechanism using MSC Adams/View, *Applied Mechanics and Materials,* Trans Tech Publications, pp. 90-97, 2014.

[12] HRONCOVÁ, D., ŠARGA, P.: Kinematics analysis of the crank mechanism conveyor Using MSC Adams, *Applied Mechanics and Materials,* Trans Tech Publications, pp. 140-149, 2015.

[13] DERVIŞ, E., ÇALIŞKAN, S.: Comparative study on the performance of different drive mechanisms used in a beta type Stirling engine through thermodynamic analysis, *International Journal of Automotive Engineering and Technologies*, Vol. 8, No. 2, pp. 44-60, 2019.

[14] DAVIDSON, A.: *Handbook of Precision Engineering: Volume 1 Fundamentals,* Macmillan International Higher Education, pp. 423, 2016.

[15] PIRNÍK, R., HRUBOŠ, M., NEMEC, D., BOŽEK, P.: Navigation of the autonomous ground vehicle utilizing low-cost inertial navigation, *Acta Mechatronica*, vol. 1, No. 1, pp. 19-23, 2016.

[16] KURYŁO, P., CYGANIUK, J., TERTEL, E., FRANKOVSKÝ, P.: Machine vision investigate the trajectory of the motion human body–review of the methods, *Acta Mechatronica*, Vol. 1, No. 2, pp. 7-13, 2016.

Review process

Single-blind peer review process.

doi:10.22306/atec.v5i4.67 *Received: 06 Dec. 2019*
Accepted: 29 Dec. 2019

SUPPLIER PLANNING WITH ANALYTICAL HIERARCHY PROCESS

Gabriela Ižaríková
Technical University of Košice, Faculty of Mechanical Engineering, Institute of Special Technical Sciences, Department of Applied Mathematics and Informatics, Letná 9, 042 00 Košice, Slovak Republic, EU, gabriela.izarikova@tuke.sk

Keywords: multiple criteria decision-making, Analytic Hierarchy Process AHP, supplier selection
Abstract: The aim of this paper is to select the optimal supplier for new equipment according to clients' selected criteria using the analytic hierarchy process (AHP). This paper is composed of a theoretical part, which constitutes a detailed methodology of the AHP an application part, in which the described method is put into practical use for ranking alternatives, the selection of the optimal supplier for a production improvement. The results of the application part are summarized in the conclusion.

1 Introduction

Nowadays is the amount of quality characteristic feature and timely information that we need to know, the optimal response is proportional to the decision we will take and from which the course of the event depends. Every day, in both business and private environments, we encounter difficult situations where decisions need to be made quickly and correctly. Multicriterial decision-making methods are often used to support and simplify decision-making, which provide an efficient apparatus for making the right decisions.

Multiple criteria decision-making (MCDM) has grown as a part of operations research, concerned with designing computational and mathematical tools for supporting the subjective evaluation of performance criteria by decision-makers [1].

Decision making is a process whereby an individual or a group (the decision maker) selects the best alternative from many possible alternatives. It represents an alternative which best meets criteria the decision maker's preferences. Among the important business activities belongs item investment decision making [2].

2 Multi-criteria decision making (MCDM)

Decision Making is the act of choosing between two or more action. Multiple-criteria evaluation problems consist of a finite number of alternatives, explicitly known in the beginning of the solution process. In Multiple criteria design problems (multiple objective mathematical programming problems) the alternatives are not explicitly known. An alternative (solution) can be found by solving a mathematical model. The number of alternatives is either infinite or not countable (when some variables are continuous) or typically very large if countable (when all variables are discrete). But both kind of problems are considered as a subclass of Multi Criteria Decision Making problems. The basic working principle of any MCDM method is same: selection of criteria, selection of alternatives, selection of aggregation methods and ultimately selection of alternatives based on weights or outranking.

Multicriterial decision-making (evaluation) depends on the choice of the appropriate method. The priority is the method, which results in the decision making based on the quantified usefulness of objects entering the decision-making process. As a result, the decision affects the relevance of the evaluation criteria, and it is therefore necessary to address procedures that allow the weighting of the evaluation criteria to be determined responsibly and accurately.

The problem of multi-criteria evaluation of alternatives is foremost a task involving finding the best (optimal) alternative and ranking the alternatives from the best to the worst conceivable. The fundamental advantages of multi-criteria decision-making methods can be found in the decision maker's ability to evaluate each alternative using many criteria. These methods compel the decision maker to express explicitly (not intuitively) his or her understanding of the importance of each criterion. Therefore, the whole process of the evaluation of alternatives becomes more transparent, easy to follow and clear, for other parties that are more or less engaged in the decision-making process as well [3].

Their common sign is that they estimate multiple options for a possible solution according to different criteria. Based on the nature and method of using the information from the evaluator, it is possible to divide the methods of multi-criteria evaluation into:

- empirical methods,
- heuristic methods,
- exact methods.

Empirical methods are using the knowledge and reality of the decision maker (brainstorming). Heuristic methods are based on subjective evaluation, the results of which are further processed exactly (neural networks). Exact methods are based on scientific analysis (statistical methods).

Multicriterial methods are widely used in decision-making or evaluation and are addressed by many experts in different fields, so approaches to these methods vary. Among the most widely used approaches to multi-criteria evaluation are those:

- Questionnaire evaluation, in which pairwise comparisons are made.
- Another approach is based on an analytical space calculation where the number of criteria reflects the number of space dimensions.
- Approach based on mathematical-statistical methods.

Several methods of multi-criteria decision-making are known - Decision Matrix Method (DMM), Forced Decision Matrix Method (FDMM), Analytical Hierarchy Process (AHP). The solution first determines the weight of the individual criteria and then quantitatively evaluates how the individual variants of the solution meet the selected criteria. The different methods differ in the method of quantification for both evaluations. The best known decision-making methods include the analytical hierarchical process (AHP) proposed by Thomas L. Saaty [4].

3 Analytic Hierarchy Process

AHP is a method designed to solve complex situations in which the most optimal decision needs to be reached. The basis of this method is divided into the multi-criteria problem, which is divided into smaller parts and then create a hierarchical model. The AHP solves multi-criteria decision-making problems based on a hierarchy. Generally, the hierarchy has three levels: the goal, criteria and alternatives. The criteria can be broken down into sub-criteria to make a lower level. AHP offers a complex and logical concept for problem structuring, the quantification of problem elements that are linked to goals and the evaluation of alternative solutions. It is widespread in several decision-making situations and areas, e.g. industry and commerce. Advantage this method comes from its variability of data evaluation, such as price, supply chain performance, quality, etc. AHP author Thomas L. Saaty was an American mathematician working as a university professor at the University of Pittsburgh [5,6].

The decision making can be structured into three levels:

- the hierarchy,
- the priority,
- the consistency.

The hierarchy

Hierarchy design is a goal definition, identification of alternatives, identification of evaluation factors, assignment of criteria and factor relationships and finishing of the hierarchy. Simultaneously with the creation of a structured hierarchy, an optimized system is developed from a group of criteria (sub-criteria) and alternatives. The most widely employed illustration of the hierarchy is shown in Figure 1.

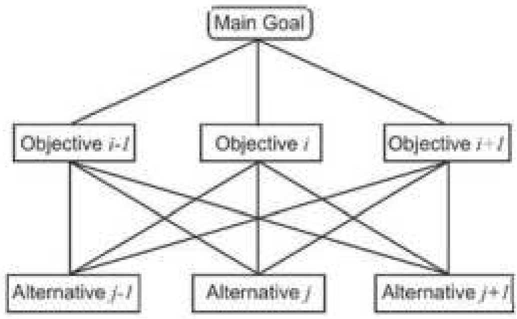

Figure 1 Structure of AHP method (hierarchy)

A hierarchy is a system of classification and organization where each element of the system, except the top one, is subordinate to one or more elements. When creating a structured hierarchy for the AHP method, an optimization system consisting of a main objective, a selected set of factors or criteria and alternatives is set up. This means that we divide the main problem into smaller separate parts. The AHP hierarchy generally has the following levels: main goal, objective (criteria) and alternatives. At the top of the hierarchy is the goal in the middle are the criteria on which we make decisions and below are the alternatives we want to decide on. The breakdown into smaller parts is very important because the evaluation of results by individual sub-criteria is easier, doubts are easier to verify [7].

The priority

Identification of priorities (application of pair-wise comparison, point evaluation of significance, repetition of the procedure for all the hierarchy levels). This step is based on the allocation of points to each paired provocation based on their degree of significance. The paired comparison method is based on the principle of comparing each criterion with each, the preference of the criterion being determined with respect to all other criteria in the set. The identification of priorities (evaluation) is based on expert estimation, in which the factor influences are compared. The scale of evaluation has five basic levels, which are mentioned in Table 1. In this scale, 1 expresses the equally preferred status and 9 expresses the extremely preferred status.

In problem solving, it is very important to assess the criteria preferences [8,9]. The more important is the criterion, the higher is its weight. A few methods exist for criteria normalization (e.g. AHP). Results of the comparison (for each factors pair) were described in term of integer values from 1 (equal value) to 9 (extreme different) where higher number means the chosen factor is considered more important in greater degree than other factor being compared with.

Table 1 The example scale for comparison

Scale-number of points	*Degree of preference*	*Descriptor*
1	Equal importance	Criteria i and j are equal.
3	Moderate importance of one factor over another	Low preference for criterion i before j .
5	Strong or essential importance	Strong preference for criterion i before j.
7	Very strong importance	Very strong preference for criterion i before j.
9	Extreme importance	Absolute preference for criterion i before j.
2, 4, 6, 8	Values for inverse comparison	Medium values between two neighbouring criteria for more precise preference determination.

The information about the significance (s_{ij}) consists of values that determine the ratio of the evaluation criterion's significance in relation to the other criteria. The elements in the matrix s_{ij} are an estimate of the weight ratios of criteria v_i and v_j, so the following applies (1). The pair-wise comparison is conducted between two criteria and the value of preference is noted in a matrix of pair-wise comparisons $S = (s_{ij})$ (2), which has a square shape (mxm). For the elements on the main diagonal of the matrix, the relationship is $s_{ij} = 1$ (each criterion is equal to itself). This matrix is reciprocal, inverse elements are determined by the following formula according to (3)

$$s_{ij} \cong \frac{v_i}{v_j} \qquad (1)$$

$$S = \begin{pmatrix} 1 & s_{12} & \cdots & s_{1j} \\ \frac{1}{s_{12}} & 1 & \cdots & s_{2j} \\ \vdots & \vdots & \ddots & \vdots \\ \frac{1}{s_{12}} & \frac{1}{s_{2j}} & \cdots & 1 \end{pmatrix} \qquad (2)$$

$$s_{ij} = \frac{1}{s_{ji}} \qquad (3)$$

Weight quantification (weighted values of alternative solutions). In the AHP weights are determined on the basis of (4), under the necessary condition of

$$\sum_{j=1}^{m} w_j = 1; \; w_i = \frac{\sqrt[k]{\prod_{j=1}^{k} s_{ij}}}{\sum_{i=1}^{k} \sqrt[k]{\prod_{j=1}^{k} s_{ij}}} \qquad (4).$$

The vector w_i is a normalized vector of weights that determines the influence of individual criteria in relation to the parent element.

The consistency

A prerequisite for a correct decision is that the rule of consistency be respected when allocating significance to individual criteria. If this is not the case, it is appropriate for the evaluating body to reconsider its rating. When many pairwise comparisons are performed, some inconsistencies may typically arise. The matrix elements are generally not absolutely consistent. However, the evaluation requires a certain level of matrix consistency, i.e. that the elements are linearly independent. That can be assessed by employing the consistency ratio (CR) as follows (5):

$$CR = \frac{CI}{RI} \;, \quad CI = \frac{\lambda_{max} - n}{n-1} \qquad (5)$$

CI is the consistency index, λ_max is the highest eigenvalue of the matrix and n represents the number of independent rows of the matrix. RI is random index that has different values for a different number of matrix criteria or alternatives, as shown in Table. 2. A consistency ratio lower than 0.1 provers the suitability of the pair-wise comparison matrix.

Table 2 Values of the random index for different numbers of criteria

N	**1**	**2**	**3**	**4**	**5**	**6**	**7**	**8**	**9**	**10**
RI	0.00	0.00	0.58	0.90	1.12	1.24	1.32	1.41	1.45	1.49

The method AHP summary consists of the creation of the hierarchy, weight quantification for each criterion (sub-criterion), comparison of the alternatives according to the identified criteria, analysis of consistency (CR) and determination of the optimal alternative (with the highest aggregate weight). The implementation steps are [10,11]:

- Determination of the problem.
- Determination of the objectives of the problem or consideration of all actors, objectives and its outcome.
- Identification of the criteria for evaluation.
- Structuring the problem in a hierarchy of different levels constituting goal, criteria, sub-criteria and alternatives.
- Comparing each element in the corresponding level and calibrate of them on the 1-9 Saaty scale.
- Performing calculations to find the maximum Eigen value, consistency index (CI), consistency ratio (CR).

The last step is to construct the priority matrix of alternatives and to calculate the overall priority vectors. The overall priority vector of each solution is calculated as

Acta Tecnología - International Scientific Journal about Technologies
Volume: 5 2019 Issue: 4 Pages: 103-107 ISSN 2453-675X

summation of the priority vector of each alternative multiplication to the respective priority vectors. The alternative with the highest overall priority value provides the result of the analysis.

4 Application

In this study, supplier selection was made for new equipment which is a production improvement. The choice was made among three suppliers. New equipment suppliers are evaluated based on selected criteria:

- C1 - Supplier price,
- C2 - The right quality (equipment),
- C3 - Warranty period provided,
- C4 - Delivery speed, Timeliness of delivery,
- C5 - Reliability of agreements.

a) Pair-wise comparison for all criteria

The priority of each decision alternative with respect to its contribution to different criteria is decided by managers group and is presented in Table 3. In this research, the intensity and importance of each criteria was chosen through a group decision. This sorted out that the supplier price and the right quality has the highest importance intensity, followed by delivery speed, timeliness of delivery while the warranty period provided and reliability of agreements has the lowest importance intensity. The consistency index, the consistency ratio and the priority vector of the synthesized matrix is presented too in Table 3.

Based on references, as presented in Table 2, for a matrix with size of 5, the random consistency ratio RI is 1.12 and the consistency ratio CR is $0.0580 \leq 0.1$. Due to the fact that CR is less than 0.1 the judgments are acceptable. Similarly, all the pair-wise comparison matrices along with the priority vectors for different criteria are calculated as presented in Table 4, Table 5, Table 6, Table 7, Table 8.

Table 3. Pair-wise comparison matrix for five criteria

criteria	C1	C2	C3	C4	C5			weights
C1	1	1	4	5	6	λ=5.2599	K1	0.4771
C2	1	1	3	2	5	CI=0.0650	K2	0.2793
C3	1/4	1/3	1	1/3	3		K3	0.0901
C4	1/5	1/2	3	1	4	CR=0.0580≈5.8%	K4	0.1082
C5	1/6	1/5	1/3	1/4	1		K5	0.0452

b) Pair-wise comparison of variants according to criteria

Table 4. Pair-wise comparison matrix for criterion C1

C1	S1	S2	S3			weights
S1	1	1/3	4	λ=3.0858	S1	0.2797
S2	3	1	5	CI=0.0429	S2	0.6267
S3	1/4	1/5	1	RI=0.58 CR=0.0739≈7.3 %	S3	0.0936

Table 5. Pair-wise comparison matrix for criterion C2

C2	S1	S2	S3			weights
S1	1	1/2	1/4	λ=3.0940	S1	0.1265
S2	2	1	1/5	CI=0.0470	S2	0.1865
S3	4	5	1	RI=0.58 CR=0.0810≈8.1 %	S3	0.6870

Table 6. Pair-wise comparison matrix for criterion C3

C3	S1	S2	S3			weights
S1	1	3	7	λ=3.0649	S1	0.6491
S2	1/3	1	5	CI=0.0324	S2	0.2790
S3	1/7	1/5	1	RI=0.58 CR=0.0559≈5.6 %	S3	0.0719

Table 7. Pair-wise comparison matrix for criterion 4

C4	S1	S2	S3			weights
S1	1	1/4	2	λ=3.1078	S1	0.2184
S2	4	1	3	CI=0.0539	S2	0.6301
S3	1/2	1/3	1	RI=0.58 CR=0.0930≈9.3 %	S3	0.1515

Table 8. Pair-wise comparison matrix for criterion 5

C5	S1	S2	S3			weights
S1	1	2	3	λ=3.0536	S1	0.5278
S2	1/2	1	3	CI=0.0268	S2	0.3325
S3	1/3	1/3	1	RI=0.58	S3	0.1396
				CR=0.0462≈4.6 %		

Table 9. Priority matrix of alternatives

Criteria	Weight	Supplier S1	Supplier S2	Supplier S3
C1	0.4771	*0.2797*	*0.6267*	*0.0936*
C2	0.2793	*0.1265*	*0.1865*	*0.6870*
C3	0.0901	*0.6491*	*0.2790*	*0.0719*
C4	0.1082	*0.2184*	*0.6301*	*01515*
C5	0.0452	*0.5278*	*0.3325*	*01396*
Weigh Sum		**0.2748**	**0.4595**	**0.2657**

Overall priority of the first supplier is 0.2748, of the second supplier is 0.4595 and of third supplier is 0.2657 and this confirms that the second supplier is the preferred solution which can satisfy the criteria (Table 9).

5 Conclusion

The article deals with a detailed analysis of the AHP method - analytical hierarchical process. It describes its origin, popularity, use to date, advantages and disadvantages which this method brings. The procedure for using the AHP method in a simple decision example is also given. The AHP is a very flexible and powerful tool because the scores, and therefore the final ranking, are obtained based on the pairwise relative evaluations of both the criteria and the options provided by the user. The computations made by the AHP are always guided by the decision maker's experience, and the AHP can consequently be considered as a tool that is able to translate the evaluations (both qualitative and quantitative) made by the decision maker into a multicriteria ranking. The AHP method is currently one of the most widely used methods of multi-criteria evaluation, because it is simple, complex, has a wide range of uses, and especially if the decision-maker enters preferential information rationally, this method gives good results. It is only necessary to know how to work with it and how to interpret the obtained data.

Acknowledgement
This work was supported by the grant projects APVV-17-0258, KEGA 001TUKE-4/2020, VEGA 1/0438/20.

References

[1] ZAVADSKAS, E.K., TURSKIS, Z., KILDIENĖ, S.: State of art surveys of overviews on MCDM/MADM methods, *Technological and Economic Development of Economy,* Vol. 20, No. 1, pp. 165-179, 2014. doi:10.3846/20294913.2014.892037
[2] FOTR, J., SOUČEK, I.: *Investiční rozhodování a řízení projektů,* Praha, Grada Publishing, 2011. (Original in Czech)
[3] FOTR, J., ŠVECOVÁ, L., et al.: *Manažerské rozhodování postupy, metody a nástroje*, Praha, Ekopress, 2010.
[4] SAATY, T.L.: *The analytic hierarchy process: Planning, priority setting, resources allocation*, New York, NY: McGraw, 1980.
[5] Thomas L. Saaty, [Online], Available: http://en.wikipedia.org/wiki/Thomas_L._Saaty [18.11.2019], 2019.
[6] Analytic hierarchy process, [Online], Available: http://en.wikipedia.org/wiki/Analytic_Hierarchy_Process [19.11.2019], 2019.
[7] STRAKA, M.: *Distribution and Supply logistics,* Cambridge Scholars Publishing, Newcastle upon Tyne, 2019.
[8] STRAKA, M.: *Distribučná logistika v príkladoch,* Dekanát - Edičné stredisko/AMS, Fakulta BERG Technickej univerzity v Košiciach, Košice, 2011. (Original in Slovak)
[9] VARGAS, L.G.: *Models, Methods, Concepts & Applications of the Analytic Hierarchy Process,* 2nd ed., Springer, New York, NY, USA, pp. 1-69, 2012.
[10] SAATY, T.L.: *Decision making with dependence and feedback: the analytic network process: The organization and prioritization of complexity,* Pittsburgh, Rws Publications, 1996.
[11] SAATY, T.L.: *Fundamentals of Decision Making and Priority Theory with the Analytic Hierarchy Process*, Pittsburgh, RWS Publications, 2006.

Review process
Single-blind peer review process.

Acta Tecnología - International Scientific Journal about Technologies
Volume: 5 2019 Issue: 4 Pages: 109-114 ISSN 2453-675X

doi:10.22306/atec.v5i4.68

Received: 12 Dec. 2019
Accepted: 30 Dec. 2019

VIRTUAL PRODUCTION TECHNOLOGY VS. ENVIRONMENT

Pavol Božek
Slovak University of Technology, Faculty of Materials Science and Technology, Institute of Production Technologies, J. Bottu 25, 917 24 Trnava, Slovak Republic, EU, pavol.bozek@stuba.sk

Keywords: robot, virtual, workplace, animation

Abstract: Specialized robotic workplaces or systems are not only a complex issue, but at the same time they are financially demanding in the field of production, especially, when the prototypes essential for mechanical engineering or forestry are concerned. Such a robotic workplace calls for an original project of a small series production and the proposed virtual environment meets the requirements for the verification of the technological properties, reliability and construct possibilities of the prototypes. The specialized robotic workplace is an interactively described 3D object and is programmable in accordance with the real environment requirements. Virtual technologies represent a convenient solution for the preparation of a safe ergonomic, economic and environmental workplace.

1 Introduction

Economic and global trends in mechanical engineering management in the Slovak Republic are heading to maintain the related EU conditions aimed at the sustainable development of the machine engineering production. These technologies related to the effectiveness of national economic development in accordance with the EU countries´ machine production management are accepted in the project phase of the new specialized robotic workplace. Authors focus on the implementation of the results in forestry.

In praxis of technology workplaces with robots the computing technology is used. It is important the used technology to be independent to platform on which it will be presented and to use the newest standards in computer technologies. The aim of our project is to design suitable technology to implement computer model of virtual technological workplace. The result will be to teach and test manipulation control operations. Virtual workplace model simulates simple logics derived from real robotized workplace.

The aim is to create fully functional virtual automated laboratory with industrial robot controlled as in praxis by personal computer.

Virtual industrial robot is for its simplicity of operation and simplicity of user access to functions especially suitable for teaching control and programming robots on various knowledge grades [1]. Also, it is possible to use it to train and examine industrial robot operators and programmers. The modelling theory is the part of larger project of virtual robotized technology workplace in laboratory conditions. Additional automated workplaces dedicated be the periphery to industrial robot will be possible to add to virtual automatized complex simulation [2,3].

2 Virtual control systems

It is obvious, that the information acquisition at real technical means of the control systems is financially demanding. The basic training for the plant and its structure´s project engineers is available at the control system supplier, and limited renewing courses at the customer´s control system. However, the principle problem lies in the operators´ preparation for emergency situations of the plant equipment. Virtual control systems connected with virtual models of control systems mean an effective solution of the abovementioned problems [4]. Current research results and further research development in the field of virtual control systems implementation are supported by VRML /Virtual Reality Modeling Language/, designed for interactive description of 3D objects and worlds.

VRML /Virtual Reality Modeling Language/ is designed for interactive description of 3D objects and worlds. It is also a universal variable format for 3D graphics and multimedia. The use of VRML can vary and comprises also the possibility of technical and scientific visualization, multimedia presentations, entertainment, computer-aided education, www pages and virtual worlds.

It is a standardized file system defined by ISO/IEC 14772. VRML is capable to represent static and dynamic (animated) 3D objects, multimedia objects with hyperlinks for individual components of multimedia, such as a text, sound, picture, animation and film. VRML was designed to meet the following requirements:

a. The possibility to create automated scripts. It allows for the development of computer programs for the VRML creation, editing and operation based on automated translation programs for the conversion of other common 3D formats into VRML files.
b. The arrangement provides the ability to combine dynamic 3D objects and VRML worlds.
c. The spreadability allows for the addition of new objects not explicitly defined in VRML
d. Performance
e. The scale allows for the development of arbitrary large dynamic 3D worlds.

The standard ISO/IEC 14772 does not need to define the physical equipment nor other concepts depending on the implementation, e.g. screen contrast or input devices. On the contrary, this standard is for wide range of equipment and implementations which do not include even a monitor /display/ or a mouse.

3 Basic principles of virtual robotized workplace

The main aim of automated laboratory modelling is simulation. It offers wide range of industrial robots use possibilities, enables to use the whole kinematics, which could not to be used in real robot because of manipulation equipment damage risk. The concept of virtual laboratory automated workplace has following advantages:

1 – decrease of risk in complicated and dangerous robot manipulations unlike in manual control,

2 – more transparency in robot control,

3 – elimination of the need to travel to the place of manipulation equipment and connected expenses,

4 – accessing the industrial robot control to students without access to control the real equipment,

5 – creating fully functional application that amends manual control in virtual form,

6 – the possibility to make various simplifications in control,

7 – instant availability at any time,

8 – the possibility to create components to expand the workplace peripheries,

9 – the possibility to work anywhere and anytime,

10 – generating of various statistic results that will be processed from any time interval of virtual laboratory work,

11 – more easily setting of work in various working modes,

12 – various periphery corrections and manipulations,

13 – exchange of gained knowledge and statistics between workers and the possibility of broader data executing,

14 – creating of own programming interface for more simplification.

Additional important positive is creation of such program automated laboratory control environment which fulfils all ecology, ergonomic and functional conditions.

4 The decision process for simulation algorithm definition

By the CNC program design as well as by the robots programming on the virtual scene, there are situations when for some machines it is necessary to wait for a defined time period. The movement speed, either angle or translation speed, represents the time function. It is essential to use the simulation algorithm controlled by events. For example: Figure 1 shows the real scene of a robotic technological workplace with the possibility to program the technological process of materials manipulation.

The training in control system real technical means is financially demanding. The basic training for the plant and its structure´s project engineer is available at the control system supplier, and limited renewing courses at the customer´s control system. However, the principle problem is represented by the operations´ preparation for emergency situations of the plant equipment. Virtual control systems connected with virtual models of control systems mean an effective solution of the abovementioned problems.

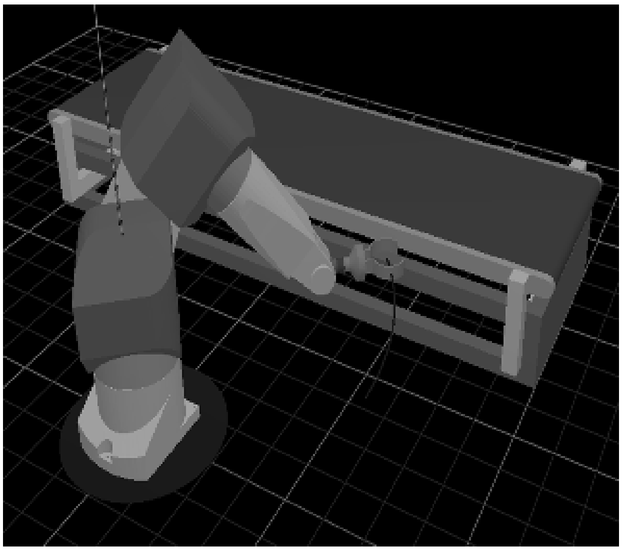

Figure 1 Virtual scene of a robotic workplace

The development process based on virtuality is at present a prerequisite for the successful process of a new product or workplace creation. In the phase of project, there exists the concept of a virtual robotic workplace model with the possibility do design real technology and define the basic principles of the technological process control system. The implementation of virtual methods in this paradigm is highly effective and leads to early decisions of real workplace effectiveness from various aspects. The original idea of a virtual technological workplace project was based on a know-how workplace. It is like the constant education level increase not only at universities - where it is necessary to implement new technologies into education.

Plant information environment as well as its system integration with the use of new IT and economic tools of IS organization and control, provides the transparency of information and knowledge processes and allows for the integration, consolidation and restructuralization of necessary information for the needs of individual plant management levels.

New trends in the IS organization and control as well as in the information and knowledge support present the creation of the whole range of new specialized functions.

They are especially informatic, economic and manager positions focused on the organizational, technical, economic and technological part of the information processes, whereas the positions focused on information processes content are missing. Drucker, a management expert, describes the lack of information responsibility. Some experts relate this field to the information and knowledge managers and comment on the difficulties with the combination of IT initiatives and knowledge management content.

The practice shows that the knowledge assurance of corporation processes calls for the need of workers interested in the information and communication processes with the emphasis on managing positions. This proves these workplaces stayed out of the system, though the work with the contents has been always the strength of IT professionals in the information databases focused on the economic growth.

Professional operator profile focused on economic and knowledge information represents an interdisciplinary problem, e.g. in the competitive intelligence or in the competences for special librarians of the 21 century for the Special library association. From the point of needs analysis, the necessary knowledge, abilities and skills are not incorporated and the information professional is missing. In the system of positions, it is necessary to create the place for an information specialist. The professional assurance of individual IS dimensions should be enhanced with the computer science, informatics, theory of information systems, information and knowledge management and information science.

Economic relations of the mentioned fields of science overlap in the professional area, though their common subject provides specialization in the assurance of plant strategic processes. It is necessary to involve the long-neglected information professionals, who are responsible for the information content, into the information and knowledge processes and consider them the key personalities of the processes.

The new possibilities of specialized robotic workplaces design, project, implementation and management allow for the simulation of the use in the project phase while meeting economic, ergonomic and sensitive environmental requirements accepted in EU countries at the same time.

It is still clear that the information acquisition in real technical means is financially demanding. The basic training for the plant and its structure´s project engineer is available at the control system supplier, and limited renewing courses at the customer´s control system. However, the principle problem is represented by the operators´ preparation for emergency situations of the plant equipment. Virtual control systems connected with virtual models of control systems offer a convenient solution of the abovementioned problems.

5 Design of actions to achieve project aims

One of additional aims is to create interface between the virtual simulation application and software interface which will directly control industrial robot by the means of hardware interface.

In the first phase the concept of project creation will be produced. Then the whole volume of work what and how to simulate will be defined. In the second phase the robotized workplace will be modelled. In this phase the actual state analysis of manipulator modes will be created and new practical functions will be designed to bypass some older non practical robot controls [5,6]. The final phase will be testing. After testing the virtual application will be used in learning.

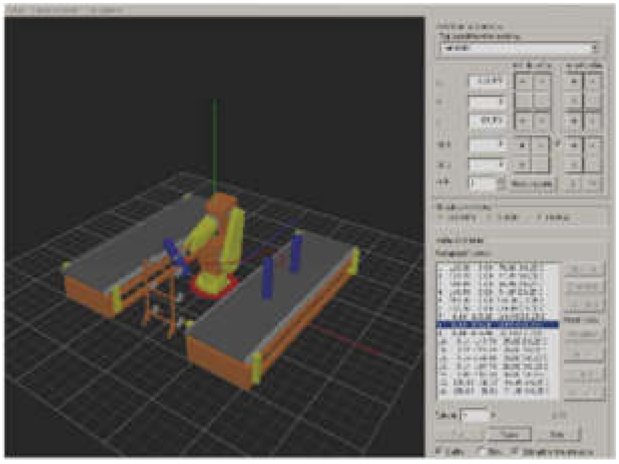

Figure 2 Virtual simulation window

The final application in Figure 2 contains virtual scene with robot in scale 1:10 and enables robot control in modes: teaching (TIN), automatic run, step by step, editing. These modes offer full control of robot's whole kinematics.

6 Application and interface

Animation as a significant part of the application illustrates the current state of all units and parts of the robotic workplace. It is impressive not only by the manual control but also by the data processing.

The animation will be carried out by the means of object-oriented Microsoft visual C+ with the use of graphic library Open GL, both providing wide possibilities of the use of a large number of orders and functions.

Library Open GL is compatible with Linux operation system and represents a standard in 3D graphics.

Interface must be compatible with the data processing generated from the virtual scene, then transformed into the real environment of a robotic workplace.

In the design phase it is important to define the interface between application and user. Additional important condition of clear control is the user not to be cluttered up with a lot of control elements. There should be few control elements and function should be clear at the first sight. In application of virtual automated workplace will be many control elements but will be ordered and integrated in the environment so that the usability will be unassuming, clear and fulfil all the user requirements.

Communication interface: in particular project parts the following standards will be used. VRML 97 for virtual scene definition, COBRA 2.0 for assigning server vs. client communication, JAVA for programming of platform independent application.
It is important to design model parameters to be possible to expand it by adding parameters.

7 Proposal of the boundary application

In the phase of the proposal of the boundary application, it is essential to define the boundary between the application itself and the application user. The ergonomics of the boundary application is an important point, i.e. the simpler the control the better. Another important condition of an application control overview is represented by the smallest possible number of control units for the user.

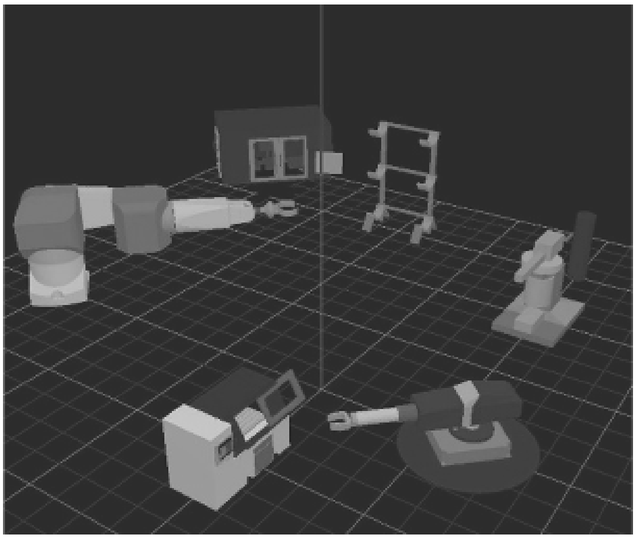

Figure 3 An example of a virtual scene creation

In the simulation application in Figure 3 of the virtual robotic workplace, there will be many control units, but they will be arranged and implemented in such a way so that they are user friendly.

It is necessary so that the application control is unified as a whole and that there is one control unit per function. Individual control units will be called by names or abbreviations and the control will be assisted by a helper.

8 The implementation of HCS model 3E in a virtual technological workplace

The concept virtual HCS model 3E of a technological workplace is designed in the phase of the project. It allows to design the technology in real as well as it permits the definition of the basic principles of the technological process control system. There are 3 acceptable aspects (3E) of sustainable development:

1 Environmental aspect - each of the technologies carry an environmental burden which also reflects to the economic aspects because of the inevitable operational measures. The advantage of the proposed virtual technology application means that it is not necessary to produce the model of a technological device, nor it is necessary to create the real technological workplace. By the production of the aforementioned devices, the environmental impact is minimized.

2 Economic aspects – there are few of them. They can be divided into partial groups and subgroups. The most important aspects that have to be in the optimization of such a technology, that are taken into consideration, are the investment costs (the amount of finances related to the specific virtual equipment purchase) and operation costs (technological devices, electricity consumption and other related costs) which can influence also the decision making in a new technology purchase.

3 Ergonomic aspects of virtual technologies – working conditions, lighting, noise, protective clothing necessary for the operation of such a technology, etc.

Work on spreading of ergonomics programs throughout Slovakia and neighbouring countries by expanding personal and completing materials for the proposed ergonomics laboratory as a part of Centre of Strategic Studies according to the proposal submitted to the scientific board of STU Bratislava, MtF.

The HCS 3E model applies the „National strategy of sustainable development of the Slovak Republic“ on the macro-level while simultaneously working on the enterprise micro-level (3E: Environmental Health, Ergonomics, Economy). This model is focusing on the effectiveness of human work and cost benefit [7]. We suppose to use this model as a tool for revitalizing the enterprises while, at the same time, revitalizing financial resources for sustainable development (Figure 4) [8].

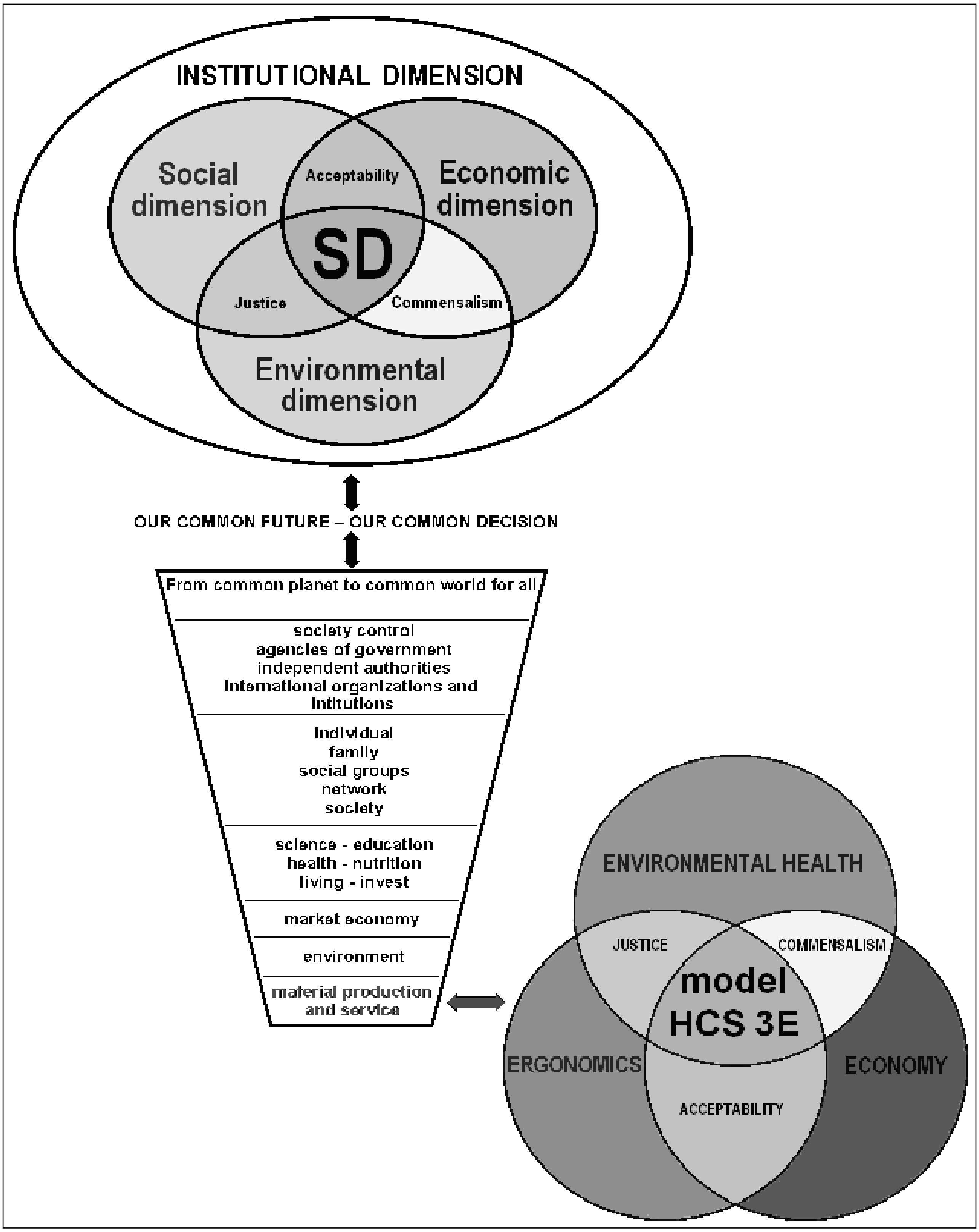

Figure 4 Model HCS 3E contribution to sustainable development (SD) – micro-solution of macro-problems

We believe this model meets our requirements in both practical and scientific areas and brings new stimuli to economic development in Slovakia and other neighbouring countries that are in the process of adapting to the conditions in the European Community.

9 Conclusion

The new possibilities of specialized robotic workplaces design, project, implementation and management allow for the simulation of the use in the project phase while meeting economic, ergonomic and sensitive environmental requirements accepted in EU countries at the same time.

It is still clear that the information acquisition in real technical means is financially demanding. The basic training for the plant and its structure´s project engineer is available at the control system supplier, and limited renewing courses at the customer´s control system. However, the principle problem is represented by the operators´ preparation for emergency situations of the plant equipment. Virtual control systems connected with virtual models of control systems offer a convenient solution of the abovementioned problems.

By keeping basic standards of information transmission and accepting enough transmission speed it is possible the student will train manipulation sequence on remote workplace. It means finance saving, it is not needed to build several robotized workplaces physical models but only model in computer and connection to software simulators.

On one hand, the various ways of environmental protection influence the economic structure, on the other hand, they create conditions for future survival of man. At the same time, they are closely related to the environmental impact caused by the technologies in mechanical engineering. Therefore, the gradual implementation of new virtual technologies is suitable as soon as in the phase of the production and technological processes begins. Now when the energy sources are limited, the mentioned technologies can win a reasonable share on the market.

References

[1] BOZEK, P., CHMELIKOVA, G.: *Virtual technology utilization teaching,* 14th International Conference on Interactive Collaborative Learning (ICL), 11th International Conference on Virtual-University (VU), Piestany, Slovakia, September 21-23, 2011.

[2] IKEUCHI, K., KANADE, T.: Automatic generation of object recognition programs, *Proceedings of the IEEE,* Vol. 76, No. 8, pp. 1016-1035, 1988. doi:10.1109/5.5972

[3] SVIATSKIY, V.M., SENTYAKOV, B.A., SVIATSKIY, M.A.: Simulation of air flow rate at point of contact with a stream of melted polymeric material, *Acta Tecnología,* Vol. 2, No. 3, pp. 1-4, 2016.

[4] ABRAMOV, I., TURYGIN, Y., SHCHENYATSKY, A., NIKITIN, Y., BOZEK, P., HALGOS, J.: *Offline Programming of Robot Model with Virtual Environment Support*, 12th International Conference on Elektro 2018, Mikulov, Czech Republic, May 21-23, 2018.

[5] FRANKOVSKY, P., HRONCOVA, D., DELYOVA, I., HUDAK, P.: Inverse and forward dynamic analysis of two link manipulator, *Procedia Engineering,* Vol. 48, pp. 158-163, 2012. doi:10.1016/j.proeng.2012.09.500

[6] QAZIZADA, M.E., PIVARCIOVA, E.: Mobile robot controlling possibilities of inertial navigation system, *Procedia Engineering,* Vol. 149, pp. 404-413, 2016.

[7] BENNAMOUN, M., BOASHASH, B.: *A vision system for automatic object recognition*, 1994 IEEE International conference on systems, man, and cybernetics - humans, information and technology, Vols 1-3, pp. 1369-1374, 1994.

[8] HATIAR, K., COOK, T.M., SAKÁL, P.: *HCS model 3E účastníckej ergonómie,* [Online], Available: https://www.google.sk/url?sa=t&rct=j&q=&esrc=s&source=web&cd=1&ved=2ahUKEwj53PDB4aHnAhWKzaQKHQzgDtYQFjAAegQIBRAB&url=https%3A%2F%2Fwww.mtf.stuba.sk%2Fbuxus%2Fdocs%2Finternetovy_casopis%2F2006%2F3%2Fhatiar.pdf&usg=AOvVaw2H0Pt1sfOt0uCJ5hy0Z3Kg [15.11.2019], 2006. (Original in Slovak)

Review process
Single-blind peer review process.

JOURNAL STATEMENT

Journal name:	**Acta Tecnología**
Abbreviated key title:	Acta Tecnol
Journal title initials:	AT
Journal doi:	10.22306/atec
ISSN:	2453-675X
Start year:	2015
The first publishing:	October 2015
Issue publishing:	Quarterly
Publishing form:	On-line electronic publishing
Availability of articles:	Open Access Journal
Journal license:	CC BY-NC
Publication ethics:	COPE, ELSEVIER Publishing Ethics
Plagiarism check:	Worldwide originality control system
Peer review process:	Single-blind review at least two reviewers
Language:	English
Journal e-mail:	**info@actatecnologia.eu**

The journal focuses mainly for the original and new, interesting, high-quality, theoretical, practical and application-oriented contributions to the field of science and research as well as to pedagogy and education in the field of technologies.

Publisher:	**4S go, s.r.o.**
Address:	Semsa 24, 044 21 Semsa, Slovak Republic, EU
Phone:	+421 948 366 110
Publisher e-mail:	**info@4sgo.eu**

Responsibility for the content of a manuscript rests upon the authors and not upon the editors or the publisher.